5-2016

Microwire regenerative peripheral nerve interfaces with wireless recording and stimulation capabilities

Ali Ajam
The University of Texas Rio Grande Valley

MICROWIRE REGENERATIVE PERIPHERAL NERVE INTERFACES WITH WIRELESS RECORDING AND STIMULATION CAPABILITIES

A Thesis

by

ALI AJAM

Submitted to the Graduate College of
The University of Texas Rio Grande Valley
In partial fulfillment of the requirements for the degree of

MASTER OF SCIENCE

May 2016

Major Subject: Electrical Engineering

MICROWIRE REGENERATIVE PERIPHERAL NERVE INTERFACES WITH WIRELESS RECORDING AND STIMULATION CAPABILITIES

A Thesis
by
ALI AJAM

COMMITTEE MEMBERS

Dr. Yoonsu Choi
Chair of Committee

Dr. Hasina F. Huq
Committee Member

Dr. Sanjeev Kumar
Committee Member

May 2016

ABSTRACT

Ajam, Ali, Microwire Regenerative Peripheral Nerve Interfaces with Wireless Recording and Stimulation Capabilities. Master of Science (MS), May, 2016, 65 pp., 1 table, 30 figures, 132 references, 13 titles.

A scalable microwire peripheral nerve interface was developed, which interacted with regenerated peripheral nerves in microchannel scaffolds. Neural interface technologies are envisioned to facilitate direct connections between the nervous system and external technologies such as limb prosthetics or data acquisition systems for further processing. Presented here is an animal study using a handcrafted microwire regenerative peripheral nerve interface, a novel neural interface device for communicating with peripheral nerves. The neural interface studies using animal models are crucial in the evaluation of efficacy and safety of implantable medical devices before their use in clinical studies.16-electrode microwire microchannel scaffolds were developed for both peripheral nerve regeneration and peripheral nerve interfacing. The microchannels were used for nerve regeneration pathways as a scaffolding material and the embedded microwires were used as a recording electrode to capture neural signals from the regenerated peripheral nerves.

ACKNOWLEDGMENTS

I would like to express my gratitude to my supervisor, Dr.Yoonsu Choi, for his patience, motivation, enthusiasm, and immense knowledge. I could not have imagined having a better advisor and mentor for my Master study. Besides my advisor, I would like to thank the rest of my thesis committee: Dr. Hasina F. Huq and Dr. Sanjeev Kumar, for their encouragement, insightful comments, and editing assistance. I would also like to thank The University of Texas Rio Grande Valley Health Science Center-Regional Academic Health Center in Edinburg (ERAHC), for all the support they have given my work. Finally, I must express my very profound gratitude to my parents for the support they provided me through my entire life. This accomplishment would not have been possible without them. Thank you.

TABLE OF CONTENTS

LIST OF FIGURES

CHAPTER I

INTRODUCTION

1.1 Problem Statement

In recent years, many scientific and technological efforts have been devoted to develop hybrid bionic systems that link, via neural interfaces, the human nervous system with electronic and/or robotic prostheses, with the main aim of restoring motor and sensory functions in patients with spinal cord injuries, brain injuries, or degenerative diseases [11]. Several designs, such as cuff electrodes, flat interface nerve electrodes (FINE) [16-18], longitudinal intrafascicular electrodes (LIFE) [16,19-21], Utah Slanted Electrode Arrays (USEA) [22-24], and regenerative sieve and microchannel electrodes [25-31] demonstrated selective recording and stimulation. However, the devices have limited electrode sites and recordings can only be obtained from the limited number of nerve fascicles. Moreover, they require advanced microfabrication techniques that not all labs have access to them and it makes the devices very expensive. A regenerative peripheral nerve interface, developed here, can be utilized to address these goals and is designed to communicate with the brain through the peripheral nervous system. Wireless stimulation and recording capabilities were also incorporated to the developed peripheral nerve interface which gave the freedom of the complex experimental setting of wired data acquisition systems and minimized the potential infection of the animals from the wire connections.

1.2 Introduction

Neural interface technologies are envisioned to facilitate direct connections between the nervous system and external technologies such as limb prosthetics or data acquisition systems for further processing. In the year 2005, 1.6 million persons were living with the loss of a limb. It is projected that the number of people living with the loss of a limb will more than double by the year 2050 to 3.6 million. One in 190 Americans is currently living with the loss of a limb. This number may double by the year 2050. Among those living with limb loss, the main causes are vascular disease (54%) including diabetes and peripheral arterial disease, trauma (45%) and cancer (less than 2%) [1]. But even though when you loss limbs, the peripheral nerves would still carry electrical command signals generated in the brain, but the signals would meet a dead end at the site of amputation and never reach the amputated muscles. So this idea encourages researchers to somehow by using the brain signals find a way to replace prosthetic limb with the loss limb. Prosthetics are changing the way amputees live, work, and function in the world. Changing technologies are providing advances in prosthetic options for arms, legs, and hands that are now easier to build, more responsive, and sometimes even cheaper than earlier options. A prosthesis is a functional replacement for an amputated or congenitally malformed or missing limb. Prosthetists are responsible for the prescription, design and management of a prosthetic device in most cases, the prosthetist begins by taking a plaster cast of the patient's affected limb. Lightweight, high-strength thermoplastics are custom formed to this model of the patient. Cutting edge materials such as carbon fiber, titanium and Kevlar provide strength and durability while making the new prosthesis lighter. More sophisticated prostheses are equipped with advanced

electronics, providing additional stability and control [2]. Prosthetics have been mentioned throughout history. The earliest example of a prosthesis ever discovered it's a toe, belonging to a noblewoman, was found in Egypt and dated to be nearly 3,000 years ago, the Egyptians were early pioneers of the idea [3]. A typical prosthetic limb costs anywhere between $15,000 and $70,000, depending on the type of limb desired by the patient. With medical insurance, a patient will typically pay 10%–50% of the total cost of a prosthetic limb, while the insurance company will cover the rest of the cost. The percent that the patient pays varies on the type of insurance plan, as well as the limb requested by the patient. For patients without health insurance, a prosthetic leg typically costs less than $10,000 for a basic prosthetic leg up to $70,000 or more for a more advanced computerized prosthetic leg controlled by muscle movements. Costs depend on the type of leg and the level of amputation. For example, a basic below-the-knee prosthetic that would allow a patient to walk on flat ground costs $5,000-$7,000, while one that would allow the patient to walk on stairs and bumpy ground could cost $10,000. For a device that would allow a patient to walk and run as well as a non-amputee, the cost could go up to $15,000. Prosthetics with special hydraulic or mechanical systems that allow for movement control can cost more than $15,000. And a computer assisted prosthetic leg costs $20,000 or more. Computerized prosthetic leg, for above the knee amputees, can cost as much as $50,000, or up to $70,000 or more, including the prosthetic foot. A prosthetic leg likely will need to be replaced several times during a patient's lifetime, and patients need ongoing adjustments. A Department of Veterans Affairs study showed the average lifetime cost for prosthetics and medical care for loss of a single leg for a veteran of the Iraq or Afghanistan wars was more than $1.4 million [4,5]. One of the advanced methods in artificial limbs is targeted muscle reinnervation(TMR) which a spare muscle of an

amputated patient is denervated then reinnervated with residual nerves of the amputated limb. The resultant electromyographical signals of the targeted muscle now represent the motor commands to the missing limb, and are used to drive a motorized prosthetic device. TMR takes advantage of intact residual nerves that previously connected to muscles distal to the amputation. The intact residual peripheral nerves are transferred to surgically denervated areas of unused musculature in the residual limb or chest (Figure 1.1). The arm and hand nerves are transferred to reinnervate the "target" muscle so that the nerves represent the absent limb physiologically. These new target muscle contractions correlate physiologically to the movements of the prosthetic device. The increased number of EMG signals enables simultaneous myoelectric control of the elbow and hand and frees the shoulder to control a powered wrist as well. The resulting control is more intuitive and thus requires less effort. Prosthetic movements are more efficient without the necessity of switching between functions. Initial outcome measure results have been very encouraging. TMR is now being performed as a clinical service, not just as a research protocol. To date, TMR programs have been developed in six different centers around the world. A critical aspect to successfully implementing TMR is the therapy that patients receive to effectively use their new prostheses. TMR is generally performed several months after the initial trauma when the residual limb has healed. The surgery involves two to four nerve transfers and is accomplished in a 2 to 5 hour operation. Details of the surgical technique are presented elsewhere [128-130]. TMR is a new technique for patients with transhumeral amputations and shoulder disarticulation. By transferring residual nerves to spare muscles, more myoelectric signals can be obtained for powered prosthesis control. TMR not only adds myoelectric control sites, but the nature of the control also contributes to easier operation of multiple joints in high-level amputations using

“offthe-shelf” components. The relationship between prosthetic arm and hand movement directly correlates with the nerve signal to the missing limb redirected to remnant muscle by the peripheral nerve transfer. Additionally, less intuitive control options remain to control added DOFs as they become available. An important goal following TMR is strengthening reinnervated muscles so they generate electrical signals that can be detected by surface electrodes. Strengthening the contraction of the transferred nerve muscles before the fitting helps the patient develop the adequate endurance needed to proceed with TMR myoelectric prosthetic training. This goal is similar to that following any amputation surgery before myoelectric control, but the exercises are different because of the redirected pathways from the brain to the host muscles. As a result, the occupational therapist (OT) must thoroughly understand peripheral nerve distribution, including which nerves are anticipated to reinnervate which muscles, to perform the appropriate strengthening exercises. About 3 weeks after surgery, the OT instructs the patient to attempt moving each missing limb joint several times daily. These exercises should be brief and relaxed attempts to move the missing hand, wrist, and elbow. These attempts may promote activity in both central brain and peripheral nerve pathways to enhance reinnervation and will prepare the patient to recognize the first signs of reinnervation. The first noticeable reinnervation usually occurs at 10 to 15 weeks after surgery; a small twitch is felt or seen in the target muscles. TMR is a technique that is becoming available to patients in more places around the world. [6].

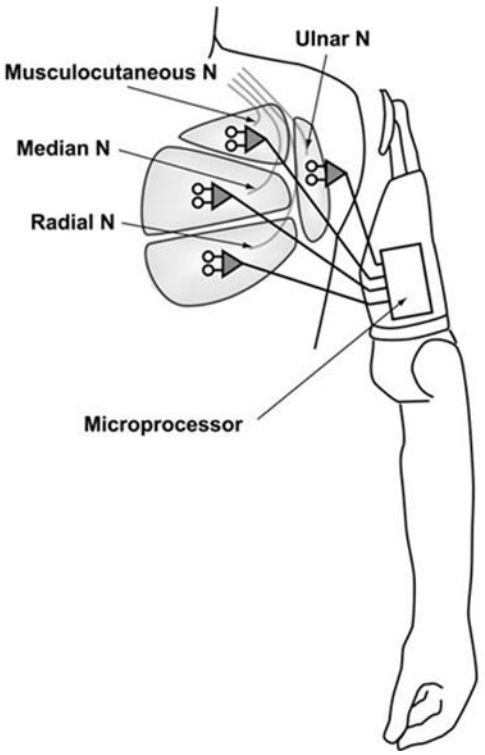

Figure 1.1: Targeted muscle reinnervation of peripheral nerves to pectoralis major in shoulder disarticulation amputation. N = nerve [6].

Despite all the advantages, researchers believe that the sensors commonly used to control robotic prostheses are too unreliable. These sensors are placed on the skin, where normal physiological processes, like sweating, can interfere with the way they work. The question is why can't we just go to the source of the information and measure the electrical signals carried in the nerves, or even the brain. The new control system works with a direct link to nerve endings and muscles in the patient. The system should provide more natural control of the arm because it allows the patient to feel what the hand is doing. Information goes both ways through the wires, both to and from the arm, and the patient gets feedback from various pressure points. The researchers believe that this is a significant step towards a more natural prosthesis, a kind of compensation for the lost arm [7]. This capability will go a long way in closing the gap between prosthetic limbs and the

natural limbs they're designed to replace. That’s why the Defense Advanced Research Projects Agency (DARPA) funds tens of millions of dollars annually to advance cutting-edge prosthetic limb technology. Their goal is to develop prosthetic limbs that approach the function of the limbs being replaced. What makes the program unique is its willingness to fund exploratory research in order to make its goal a reality as soon as possible [8]. Having some information about the peripheral nervous system and central nervous system can help the understanding of this method. A nerve provides a structured pathway that supports the electrochemical nerve impulses transmitted along each of the axons. In the central nervous system, the analogous structures are known as tracts. Neurons are sometimes referred to as nerve cells, although this term is misleading since many neurons do not occupy nerves, and nerves also include non-neuronal support cells that contribute to the health of enclosed neurons. Each nerve is a cable-like structure that contains many axons that are sometimes referred to as "fibers. " Within a nerve, each axon is surrounded by a layer of connective tissue called the endoneurium. The axons are bundled together into groups called fascicles. Each fascicle is wrapped in a layer of connective tissue called the perineurium. Finally, the entire nerve is wrapped in a layer of connective tissue called the epineurium. The endoneurium consists of an inner sleeve of material called the glycocalyx and a mesh of collagen. Nerves are bundled along with blood vessels, which provide essential nutrients and energy to the enclosed, and metabolically demanding, neurons. Within the endoneurium, individual nerve fibers are surrounded by a liquid called the endoneurial fluid. The endoneurium has properties analogous to the blood-brain barrier. It prevents certain molecules from crossing from the blood into the endoneurial fluid. In this respect, endoneurial fluid is similar to cerebro-spinal fluid in the central nervous system. During nerve irritation or injury, the amount of endoneurial fluid may increase at the site of damage. This increase in fluid can be visualized using

magnetic resonance neurography to diagnose nerve damage [9].

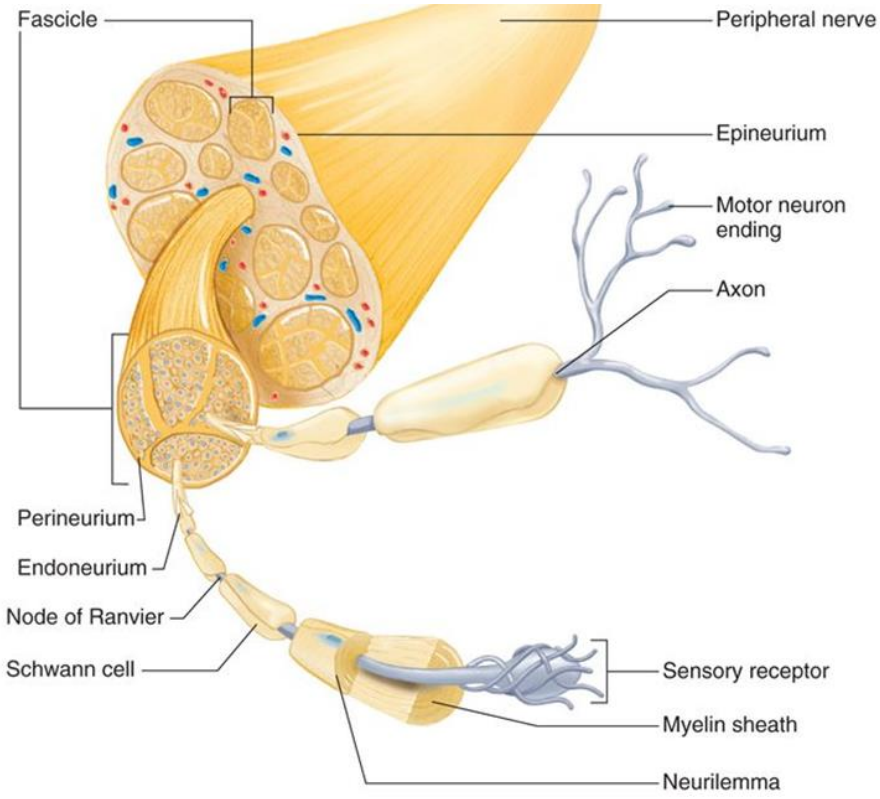

Figure 1.2: Cross section view of peripheral nerve [131].

The blood supply to nerves is provided by coiled segmental arteries that enter the epineurium periodically along the length of the nerve and form the vasa nervorum. Arteries divide into epineurial arterioles that form an anastomotic network running primarily longitudinally within the epifascicular epineurium and the interfascicular epineurium. Epineurial arterioles are supplied with a perivascular plexus of serotoninergic, adrenergic, and peptidergic nerves. Perforating arterioles cross the perineurium at oblique angles and carry a short sleeve of perineurial cells into

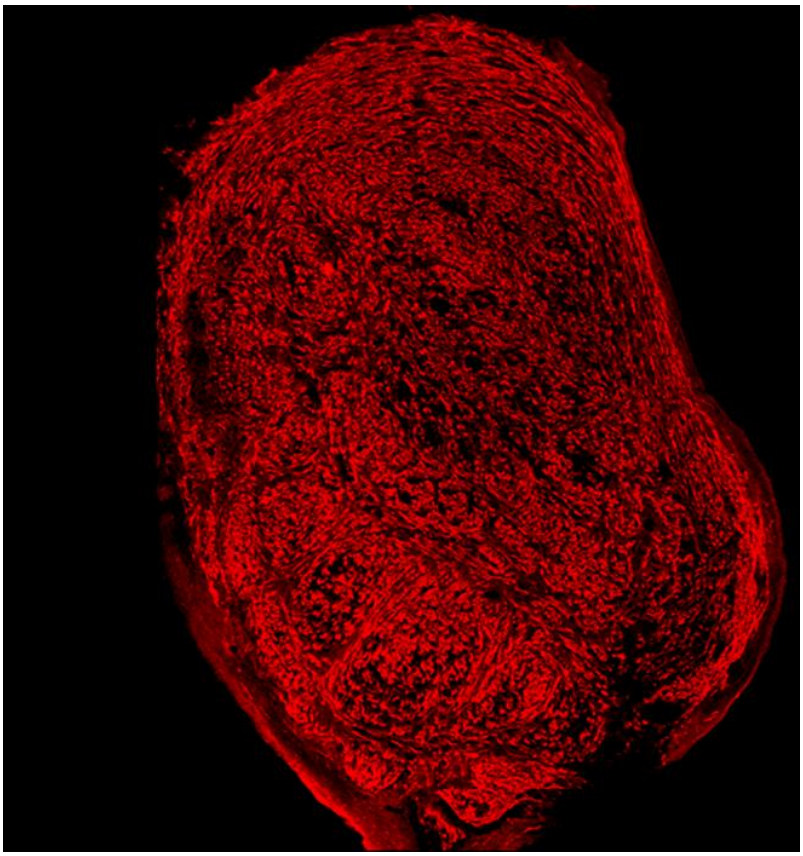

Figure 1.3: confocal microscopy image of peripheral nerve (Cross section view).

the fascicle. Perineurial arterioles have poorly developed smooth muscle and thus have limited ability to regulate intrafascicular blood flow. Within the endoneurium, arterioles immediately turn into large-diameter, longitudinally oriented capillaries that allow blood flow in either direction. The endothelial cells of endoneurial capillaries are connected by tight junctions, thus forming the tight blood-nerve barrier. Venules return blood to the venous system. Of note, lymphatic capillaries are present only within the epineurium; there is no lymphatic drainage from the intrafascicular or endoneurial space [10].

(Figure 1.2) and (Figure 1.3) illustrate the structure of peripheral nervous system. In recent years, many scientific and technological efforts have been devoted to develop hybrid bionic systems that link, via neural interfaces, the human nervous system with electronic and/or robotic prostheses, with the main aim of restoring motor and sensory functions in patients with spinal cord injuries, brain injuries, or degenerative diseases [11]. Although cultured in vitro neuronal networks have shown a variety of mechanisms of neuronal functionality, the major role of behavioral control by the nervous system cannot be incorporated with the in vitro neuronal networks system. Neuronal interface signals captured from awake, freely behaving animals are crucial for the next level of clinical applications. In amputees, such technologies would provide direct neural control of prosthetic movements and restore sensory feedback by functionally reconnecting damaged efferent motor and afferent sensory pathways. The peripheral nerve has been one target for bidirectional interfacing, with renewed interest generated by reports that peripheral nerve tissue is viable for interfacing even years after injury or amputation [12-15]. Several designs, such as cuff electrodes, flat interface nerve electrodes (FINE) [16-18], longitudinal intrafascicular electrodes (LIFE) [16,19-21], Utah Slanted Electrode Arrays (USEA) [22-24], and regenerative sieve and microchannel electrodes [25-31] demonstrated selective recording and stimulation. Microelectrode devices that contact peripheral nerves or muscles using an electrical coupling method are the most common and best known type of interfacing device [11]. Microneurography has widely been used in humans as one of the low invasive methods for the measurement of multiunit peripheral nerve activity and has become an invaluable tool for investigating somatosensory, motor and autonomic physiology and pathophysiology [32]. Usually, a tungsten microelectrode is inserted percutaneously into fascicles of limb and facial peripheral nerves of conscious human subjects to monitor activities of afferent or efferent nerve fibers. Unitary

recordings of practically all types of nerve fibers have been studied and reported. Despite the production of microlesions caused by the electrode insertion into the nerve, the morbidity with the procedure is acceptably low [33]. Microstimulation through the electrode can be used to activate single axons, although in most cases stimulation affects small groups of axons in the fascicle [34]. An interesting study used a microelectrode to stimulate the sensory nerve of an operator to indicate contact with an object by a remote robotic hand [35]. However, the use of multiple wire needles for interfacing a high number of nerve fibers has practical problems for long-term use. In acute experiments, multiple-wire-microelectrode arrays were inserted into rat nerves to investigate selective stimulation of motor units [36]. Although involving a more invasive insertion procedure, electrode arrays provided neural contacts with low-force recruitment properties similar to those of single wires. Array results revealed partial blocking of neural conduction, similar to that reported with microneurographic insertion with single needles. The arrays were capable of evoking threshold forces selectively with high efficiency. Motor recruitment was found more stable with stimulation by intrafascicular multielectrodes than by extraneural electrodes. Especially for intrafascicular electrodes, no strict inverse recruitment was observed [37]. Multielectrodes that carry a variable number of electrode sites mounted on a needle or incorporated in glass, silicon, or polyimide carriers have been developed in 1D, 2D, or 3D arrays (Figure 1.4). Different design approaches and fabrication techniques including precision mechanics and micromachining techniques have been introduced for multiunit electrodes [38-43], and some can be supplied with onboard microelectronics. Although primarily designed and used as CNS interfaces, some have also been tested as PNS interfaces. Because implanting such devices is associated with potential damage to the nervous tissue, especially if the substrate is stiff, efforts have been directed at miniaturizing the penetrating portion, developing insertion devices, and

using flexible substrates. Silicon-based shaft microprobes have been produced for years at the Center for Integrated Sensors and Circuits of the University of Michigan, leading to a large number of single-shaft, multishaft, or 3D stacked multishafts [38,44-47]. These probes are fabricated using advanced microfabrication techniques also employed in the semiconductor industry. The substrate is either needle- or wedge-shaped to allow penetration in the nervous tissue. Thus, recording or stimulation affects axons not only at surface locations but also at defined depths where active sites are placed in the electrode. Shaft electrodes allow great flexibility in their application in acute experiments but are not easy to use in long term experiments and are difficult to insert in peripheral nerves. A silicon based ribbon electrode with high flexibility demonstrated successful function after chronic implantation of up to one year [44], but this interconnect cable was not designed for implants in the highly mobile somatic peripheral nerve and was too stiff and brittle for intrafascicular application [48]. Multichannel silicon microelectrodes were implanted in several acute and chronic preparations within the cochlear nerve of animals for auditory stimulation. They induced stimulation with thresholds substantially lower than with scala tympani electrodes and with a high degree of specificity [49]. Nevertheless, the loss of neurons in spiral ganglion and cochlear nucleus was found, thought to be due to difficulty with electrode insertion and chronic motion of the implants. Silicon probes with multiple electrode sites have been recently tested for microstimulation of the sacral spinal cord for bladder contraction [50]. Highly flexible polyimide-based devices have been developed for interfacing peripheral nerves [51,52], but they have not been fully tested for intrafascicular nerve recording and stimulation. Separate research groups from the University of Utah and the University of Twente fabricated multielectrode arrays (MEAs) with 100 or more needle shaped electrodes in silicon or silicon-glass technology for neural applications. Most of the long

experience with MEAs involves their use as cortical interface [53]. Silicon glass technology has been used to produce 3D arrays of 128 electrodes with varying height from 250 to 600 μm [54,55]. In a series of experimental and modeling studies, Rutten and colleagues concluded that an electrode separation of 120 μm was optimal for selective interfacing peripheral nerves, such as the rat peroneal containing around 350 alphamotor fibers [56]. Thus, a trade-off must be made between selectivity of stimulation and the total number of nerve fibers that can be activated; optimal selectivity requires the use of redundant electrodes in the 3D configuration [54]. Intraneural Utah MEAs made of silicon with 25 and 100 individual needle electrodes have been inserted into a peripheral nerve in experimental animals using a pneumatic insertion device without significantly disturbing nerve function. To decrease the number of redundant electrodes and provide access to more fascicles within the nerve, a slanted array with electrodes of varying length, ranging from 0.5 to 1.5 mm with 0.1 mm difference in length between rows of neighboring electrodes, has been developed [57]. Electrodes in the array were capable of selectively recording single-unit responses from mechanoreceptors, although only in 10–20% of the electrodes, and evoked graded recruitment of force in muscle groups in a highly selective fashion with current injections in the 1–20 mA range [57,58]. Recruitment curves for the electrode array were broader with twitch thresholds starting at much lower currents than usual for cuff electrodes. Both the recording and stimulation were stable over the 36-h-long period of the experiments. However, the rigid structure of such electrodes and the tethering forces produced by the lead wires may induce problems when applied to limb nerves. Electrodes without and with lead wires were implanted for up to 7 months in cat sciatic nerves [59]. The surgical technique highly affected the long-term results. The stimulation properties stabilized in 80% of the electrodes over the course of the experiment, but the recorded sensory signals were not stable over time. A histological analysis

indicated that the morphology and fiber density of the nerve around the electrodes were normal. The Utah MEA is also capable of recording more effectively from more dorsal root ganglion neurons than has been achieved by conventional recording techniques, providing a more stable option for chronic implantation [60]. A case report on a healthy volunteer who had a MEA implanted in the median nerve for three months gives support to the potential of such devices for bidirectional interfacing the PNS [61]. The subject received feedback information from force and slip sensors in a prosthetic hand and subsequently used the array to control the hand for grasping an unseen object. One negative aspect was the gradual degradation of the electrode wire bundle.

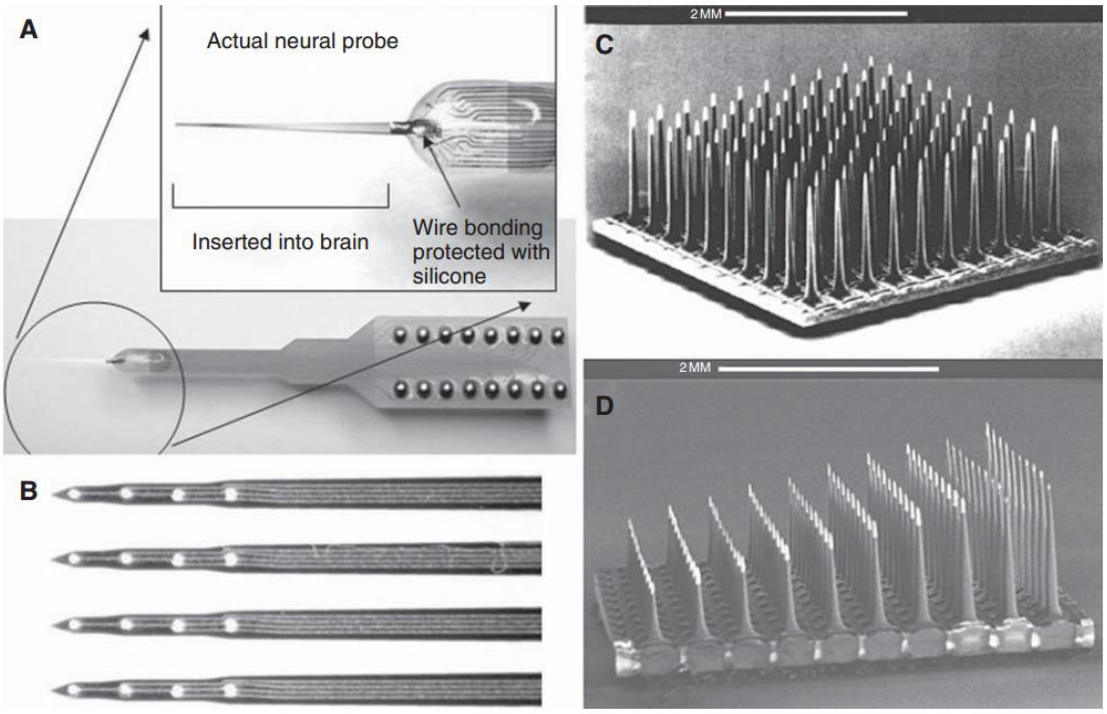

Figure 1.4: Penetrating electrodes developed at the University of Michigan (left) (from Neuronexus Inc.) and at the University of Utah (right) [57,60].

Regenerative electrodes are another kind of electrodes that are being used by researches recently. Regenerative electrodes are designed to interface a high number of nerve fibers by using an array of holes, with electrodes built around them, implanted between the severed stumps of a peripheral nerve [61-64]. Regenerating axons eventually grow through the holes (Figure 1.5), making it possible to record action potentials from and to stimulate individual axons or small fascicles. Applicability of regenerative electrodes is dependent on the success of axonal regeneration through the perforations or holes, the possibility of nerve damage from the mechanical load imposed by the electrode or from constrictive forces within the holes, and the biocompatibility of the components [65-66]. Different techniques and materials have been used during the last 30 years in the construction of regenerative electrodes. Early electrodes were made from non-semiconductor materials by mechanically drilling holes into epoxy modules [67].

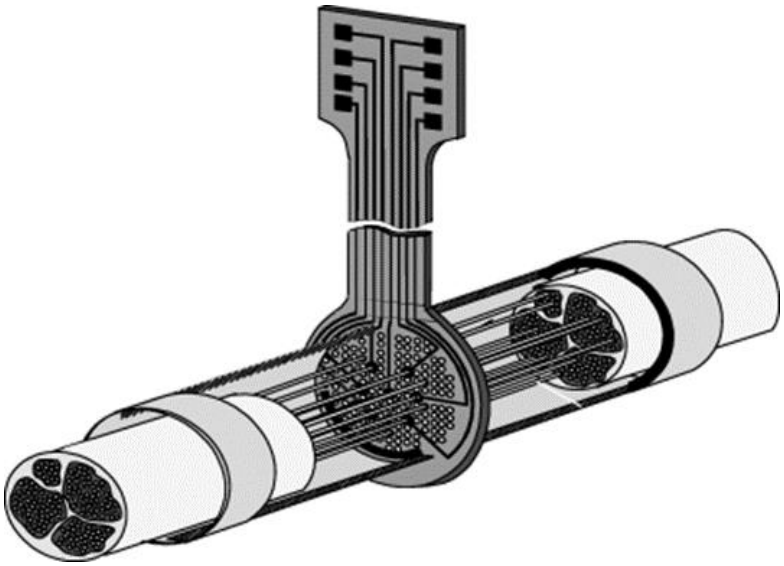

Figure 1.5: Schematic concept of a regenerative electrode. Nerve fibers of a sectioned nerve grow through the holes of the electrode encased in a guidance tube [93].

With the advent of microelectronic technologies, it became possible to construct silicon electrodes with smaller dimensions and higher number of holes (Figure 1.6) [66,68-70]. Using multiple-hole silicon arrays, the researchers demonstrated axonal regeneration and even neural activity recording was demonstrated in peripheral nerves of rat, frog, and fish [66,69,71-73]. However, such silicon interfaces cause frequent signs of axonopathy and constitute a physical barrier that limits the elongation of regenerating axons depending on the size of the holes [62,65,66,74]. Ideally a one-to-one design would allow access to each individual regenerated axon grown through one hole (2–10 μm in diameter). However, this has been proved impossible; nerve regeneration fails with holes of such small size. An equilibrium should be considered between the number of holes in the dice and their diameter in the range of 40–65 μm. More adaptive polyimide based electrodes were introduced more recently [52,75]. Polyimide can be micromachined in various designs suitable for implantation (Figure 1.7). Polyimide-based electrodes have been shown to be biocompatible and stable over months of in vivo implantation and allow for much better regeneration than silicon dice [75-77]. The presence of a polyimide-based regenerative electrode showed no chronic foreign body response, and the immunohistochemically measured pattern of characteristic proteins was comparable with a healing reaction without any implant [78]. Modifications of the structure have been suggested including an increase in the diameter of holes and enlarging the total open area within the sieve electrode in order to facilitate regeneration of a larger number of axons and to reduce potential chronic damage to regenerated axons. In parallel with technological advances, neurobiological strategies need to be investigated and applied to enhance regeneration of motor axons and to rescue regenerated axons from compressive forces [77,79]. No human implants of regenerative electrodes have been reported. One of the most logical and challenging applications of regenerative electrodes consists of their

implantation in severed nerves of an amputee's limb for bidirectional interface in a feedback-controlled neuroprosthesis. On the one hand, recording of neural efferent signals can be used for the motion control of a mechanical prosthesis [62], and on the other hand, sensory feedback from tactile and force sensors might be provided to the user through stimulation of afferent nerve fibers within the residual limb [80].

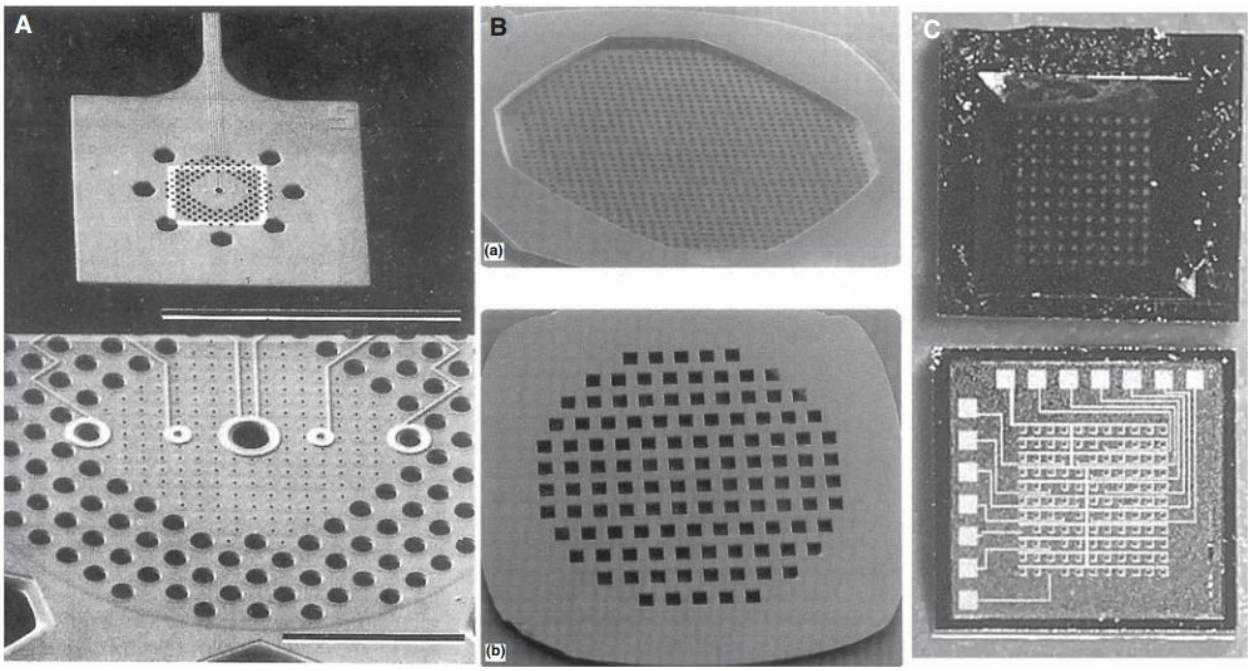

Figure 1.6: Examples of regenerative sieve electrodes made on silicon developed at the University of Michigan (A) [69], the University of Lund (B) [71], and the Microelectronics National Center (C) (CNM, Barcelona).

Unfortunately, multichannel regenerative electrodes can be applied only to transected nerves and some time is needed for interfacing the regenerated axons, thus precluding acute experiments. From chronically implanted regenerative electrodes, it has been possible to stimulate different nerve bundles and to record nerve action potentials in response to functional stimulation [75,76], although technical difficulties have to be taken into account. The limits on the amplitude and

discriminability of single-unit action potentials recordable from nerve fibers inside tubular electrodes [81] may also apply to regenerative electrodes, thus decreasing the actual amplitude of recorded signals. The fact that the electrodes are placed around instead of parallel to the nerve fibers, the size and length of each electrode hole, and the smaller than normal diameter and internodal length of regenerated fibers should be considered in further studies. A simpler alternative procedure for the extraction of information from lesioned nerves for use in the control of prosthetic devices has been described. Amplified motor signals can be obtained from lesioned nerves by allowing them to innervate isolated slips of host muscle, from which EMG signals can be recorded by wire electrodes [82].

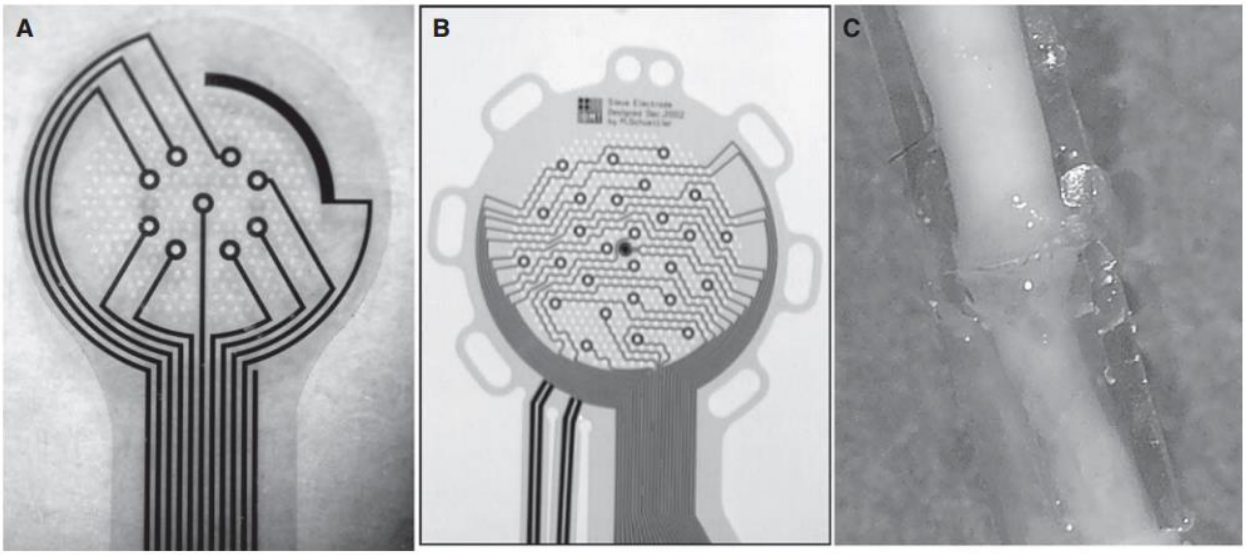

Figure 1.7: Polyimide sieve electrodes (A and B) developed at IBMT. The black lines and circles correspond to the platinum deposited contact electrodes. Micrograph of a regenerated nerve through a polyimide sieve electrode (C) [93].

Further work is required to determine the long-term stability of the interface with respect to innervation by the foreign nerve, signal characteristics, and the fidelity of the signals to reflect the motor activity of muscles originally denervated. This method has been applied in a patient with upper arm amputation in whom residual brachial plexus nerves were anastomosed to pectoralis

muscles. The few reformed motor units allowed for the simultaneous control of two degrees of freedom with a myoelectric prosthesis [83]. However, the devices have limited electrode sites and recordings can only be obtained from the limited number of nerve fascicles. Moreover, they require advanced microfabrication techniques that not all labs have access to them and it makes the devices very expensive. A regenerative peripheral nerve interface, developed here, can be utilized to address these goals and is designed to communicate with the brain through the peripheral nervous system. Previously, we developed 4-electrode and 8-electrode microwire regenerative peripheral nerve interfaces (μPNI) [84-89]. Here we report an advanced generation of the 16-electrode μPNI and even further advanced the μPNI with wireless communication capabilities. (Figure 1.8) and (Figure 1.9) shows the cross section view of our device.

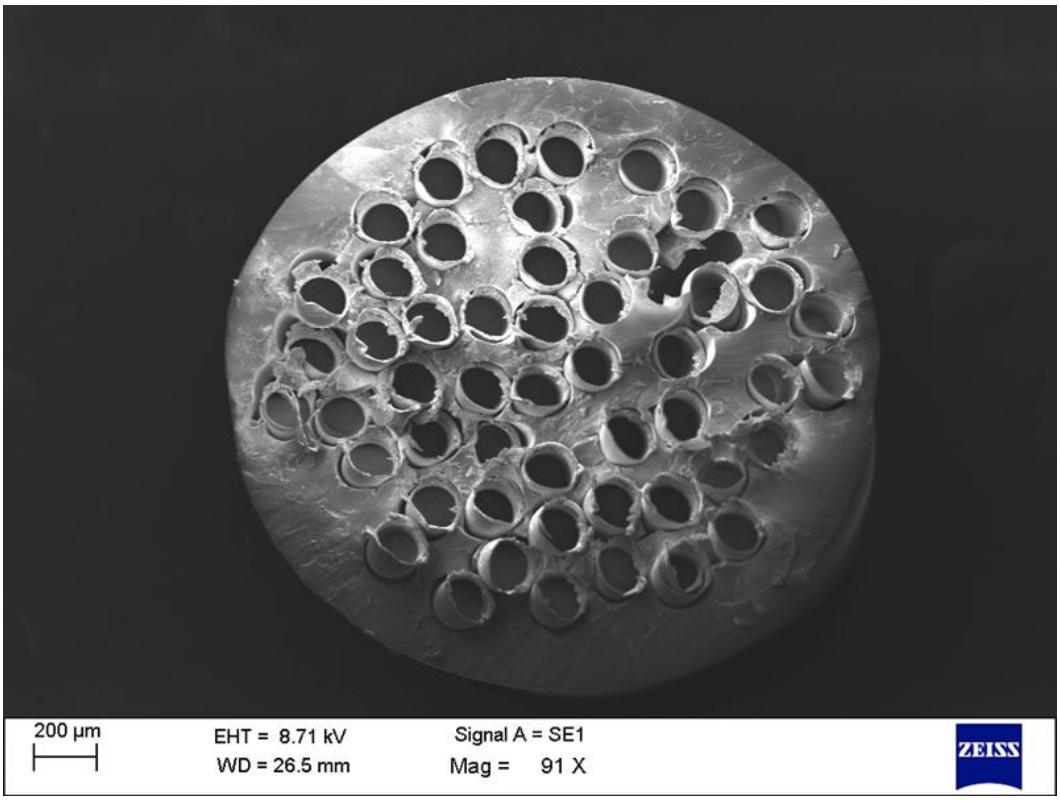

Figure 1.8: Transmission electron microscopy (TEM) image of the side with 50 microchannels.

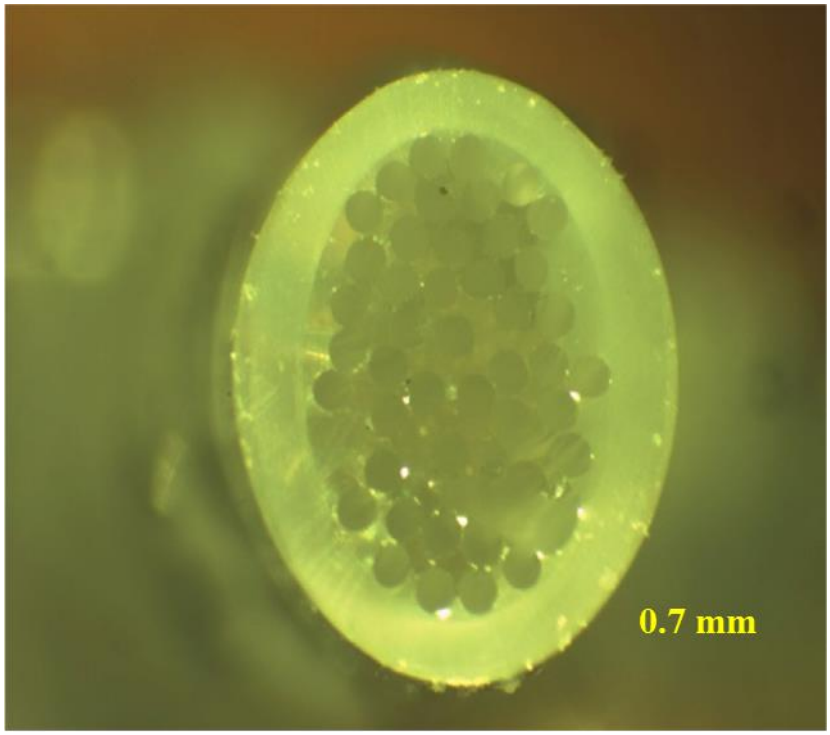

Figure 1.9: Resultant cross-sections with 50 microchannels.

Wireless stimulation and recording capabilities gave the freedom of the complex experimental setting of wired data acquisition systems and minimized the potential infection of the animals from the wire connections. The whole implantable microdevice nerve grafting involves directly suturing both ends of the affected nerve with a donor nerve, traditionally the sural nerve [19]. Although nerve grafting has proven to be an effective method in numerous cases, it does critical concern becomes inevitable when having an injury affecting multiple nerve paths which can be problematic and has greatly limit its medical and technological applications. consists of a μPNI for recording placed on the transection site of the sciatic nerve, and three μCuff electrodes, one for stimulation placed on the proximal site of the transection site of the sciatic nerve and the other two for recording placed on the tibial nerve and the common peroneal nerve. Additionally, two

electromyography electrode pairs were implanted on the tibialis anterior (TA) and soleus (SOL) muscles on the right hind leg to record the muscle signals during animal's locomotion tests. It gives us the capability of both electrophysiological recording and stimulation to develop a communication pathway from the brain to the endings of peripheral nerves. Peripheral nerve stimulation from one end of the μPNI initiates a neural signal pathway. Animal locomotion on a treadmill was tested in the animal facility at UTRGV and the μPNI has enabled us to analyze any sophisticated behavioral patterns. There are three fundamental neuroscience backgrounds correlated with the μPNI (Table 1). Independent microchannel neural interfaces will be creatively achieved by microwires embedded inside the microchannel scaffolds which can be occupied by regenerated nerve and develop an isolated neural signal communication. Along with peripheral nerve regeneration, the microwires on the nodes of Ranvier can cover and record neural signals selectively from an isolated neural signal source.

Neuroscience Fundamentals	**μPNI**
Peripheral nerves regenerate (like hair and nails)	Custom designed Microchannel Scaffolds support nerve regeneration
Action potentials are recordable every 1mm from nodes of Ranvier	1.0 mm length open microwire Electrodes in 3 mm length microchannel scaffolds
CNS-PNS neurons are connected from the brain to peripheral nerves	Peripheral Nerve Interface will collect details of the Brain making the process Noninvasive Brain-Machine Interfaces

Table 1: Supports from neuroscience fundamentals.

The microchannel and microwire are long enough to cover and record neural signals from the isolated nerve branch by structural selectivity during nerve regeneration. A commercially available wireless recording system was efficiently adopted to the peripheral nerve interface. The 32-channel wireless recording system covered 16-electrode microwires in the peripheral nerve interface, two cuff electrodes, and two electromyography electrodes. The 2-channel wireless stimulation system was connected to a cuff electrode on the sciatic nerve branch and was used to make evoked signals which went through the regenerated peripheral nerves and were captured by the wireless recording system at a different location. The successful wireless communication was demonstrated in the result section and the future goals of a wireless neural interface for chronic implants and clinical trials were discussed together.

1.3 Thesis outline

This thesis is divided into 6 chapters. Chapter 1 describes previous work and gives motivation for the works performed in this thesis. Chapter 2 presents the fabrication procedure and the materials that have been used to make the handcrafted peripheral nerve interface. Chapter 3 presents the surgical procedure and describes how we implanted the micro peripheral nerve interface. Chapter 4 presents the experimental results and the significance of the result. Chapter 5 presents the histology process that confirms the successful implantation of the device. Chapter 6 summarize the main conclusion of this thesis and presents an outlook for future work.

CHAPTER II

FABRICATION PROCEDURE

Microfluidic channel scaffolds were developed to direct peripheral nerve growth. 50 wires (160 μm in diameter) were tightly packed into Silastic® tubes (OD 1.96 mm, ID 1.47 mm; Cat. No. 508-006, Dow Corning, MI) and then were cast in liquid PDMS (Sylgard® 184, Dow Corning, MI) with a 10:1 base to curing agent ratio. They were placed in a vacuum chamber until all air dissipated (Figure 2.1), if there is still a significant amount of air bubbles within the shell, an additional degassing is recommended using horizontal vacuuming just like (Figure 2.2 (a)), which consists of placing the sample in the aluminum foil boat filled with PDMS.

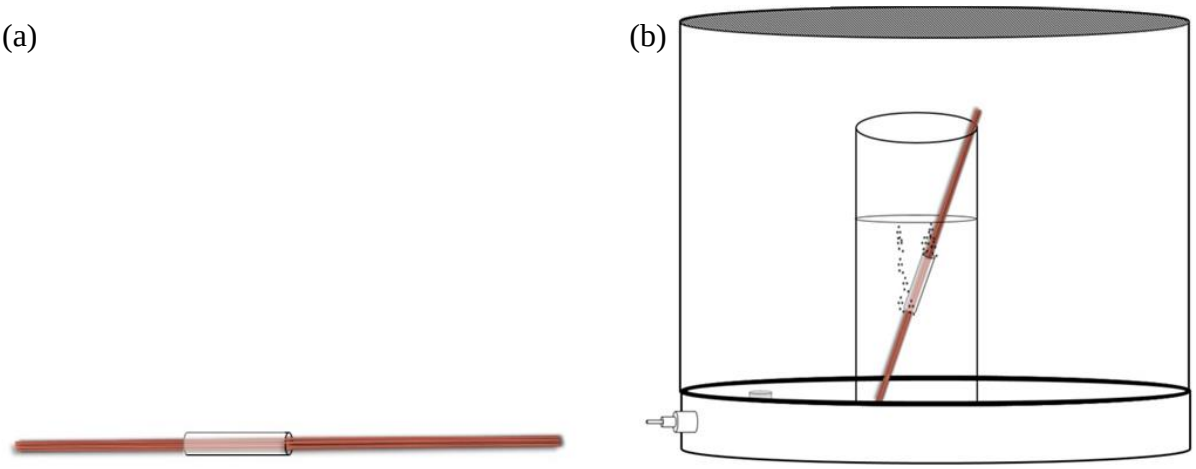

Figure 2.1: (a) 50 wires packed into Silastic, (b) the structure were cast in liquid PDMS and then placed in a vacuum chamber until all air dissipated.

If still air bubbles are found inside the shell, they should be taken out immediately by using the tweezers under the microscope. At the other end of each bundle the wires were slightly twisted and soldered together to a flat surface of a metal block this is in order to transfer the heat from oven to PDMS inside the shell. (Figure 2.2 (b)).

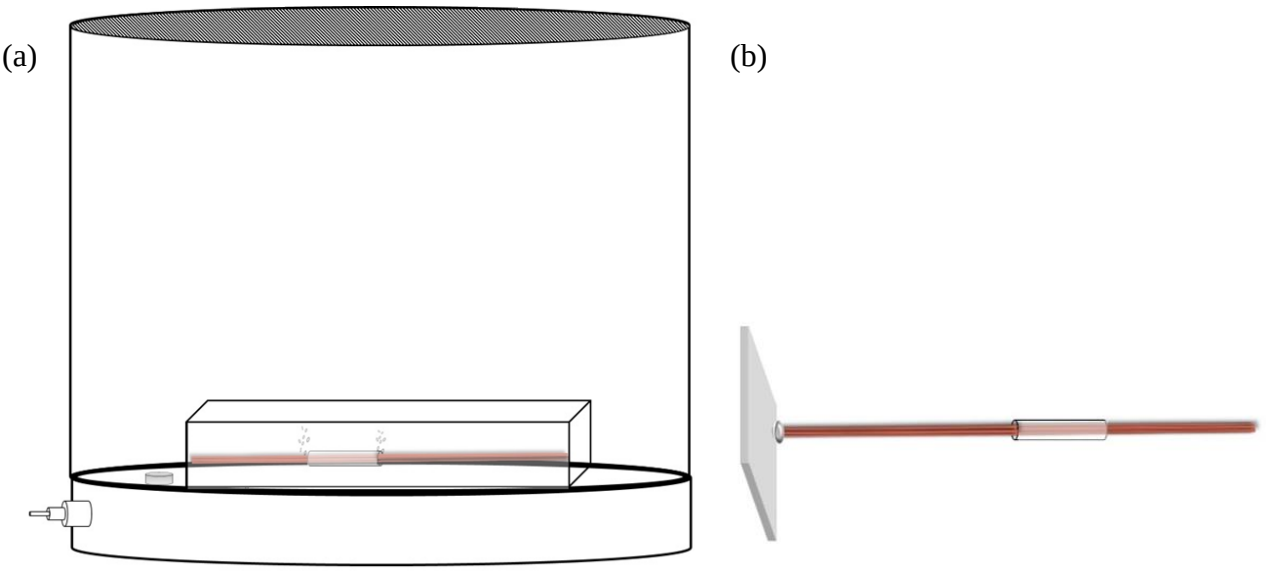

Figure 2.2: (a) Horizontal vacuuming, (b) Twisted wires soldering on metal block

After soldering the structure were placed in an oven for 2 hours at 90ºC to allow the liquid PDMS to solidify (Figure 2.3 (a)). The Silastic® tube and Sylgard 184® are composed of the same PDMS material and became a single structure as the liquid PDMS solidified. The solidified PDMS was soaked in chloroform, causing it to expand (Figure 2.3 (b)). The wires were henceforth, removed leaving behind a long, flexible scaffold with an array of microchannels within it. Chloroform is a highly volatile solvent, leaving no residue when it is evaporated. No special process is required for the fabrication process to clean chloroform. Chloroformswollen PDMS was switched into 70% ethanol to clean the device while shrinking down PDMS and run sterilization process together.

(a) (b)

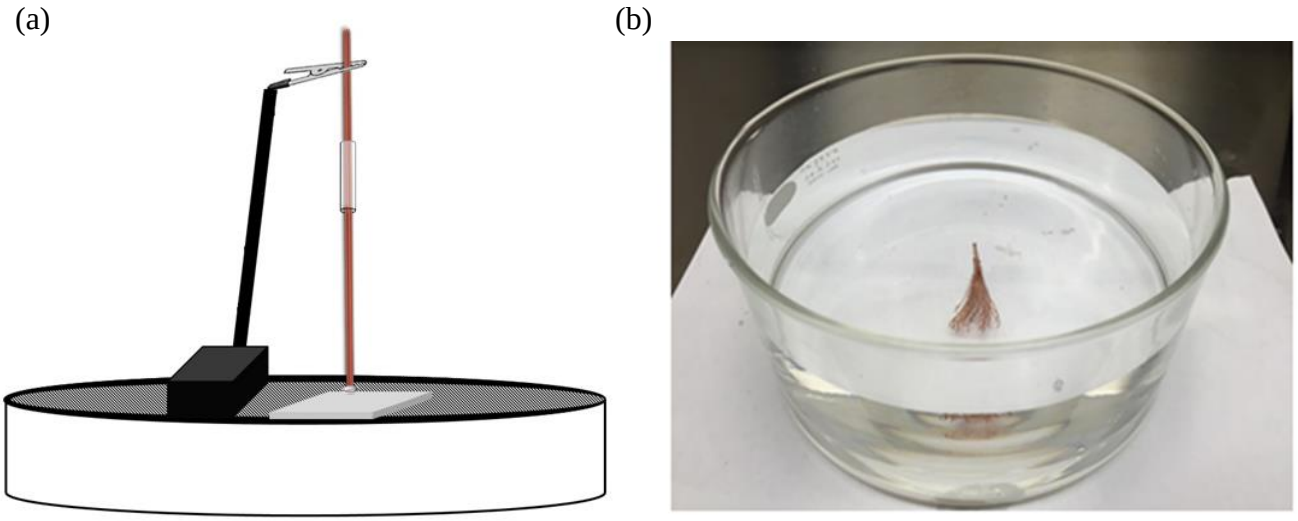

Figure 2.3: (a) Curing of PDMS in the Thermo Scientific Oven for 2 hours, (b) The sample is submerged in a chloroform.

PDMS scaffolds were placed in an oven at 100°C for 20 minute to make any remaining Chloroform evaporate. The 75 μm diameter microwires (Stablohm 800A, California fine wire, Grover Beach, CA) were inserted in the 160 μm diameter microchannels to record the neural signals from the regenerated nerves inside microchannels. No special micromachining equipment was required and commercially available microwires were efficiently used to implement the μPNI structures. Once the PDMS scaffolds were fabricated, commercially available microwires (75 μm diameter) were embedded within their microchannels. The scaffold was cut 3 mm lengthwise (Figure 2.4 (a)) and PDMS tubes, used as suture guides, were placed at both proximal and distal ends of the scaffold, hereafter referred to as proximal and distal tubes, respectively. The proximal tube was cut 3.5 mm long and placed on one end of the scaffold, thereby covering 1.4 mm of the scaffold. It was secured to the scaffold by placing a drop of liquid PDMS solution where they make contact (on the outer surface of the scaffold) and placing in an oven at 90°C for 10 minutes. The distal tube was cut 4 mm long and placed so that it covered 1.4 mm of the other end of the scaffold (Figure 2.4 (b)). To

assist in the process of embedding microwires in the scaffold, a small circle with a slit leading to it was made in the distal tube (Figure 2.5 (a)).

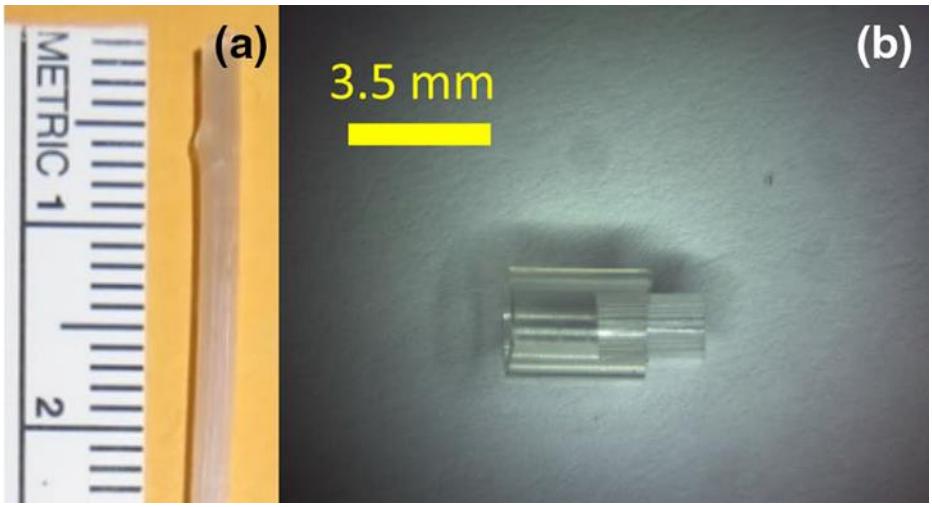

Figure 2.4: (a) 3 mm lengthwise of scaffold, (b) PDMS tubes for suture guides.

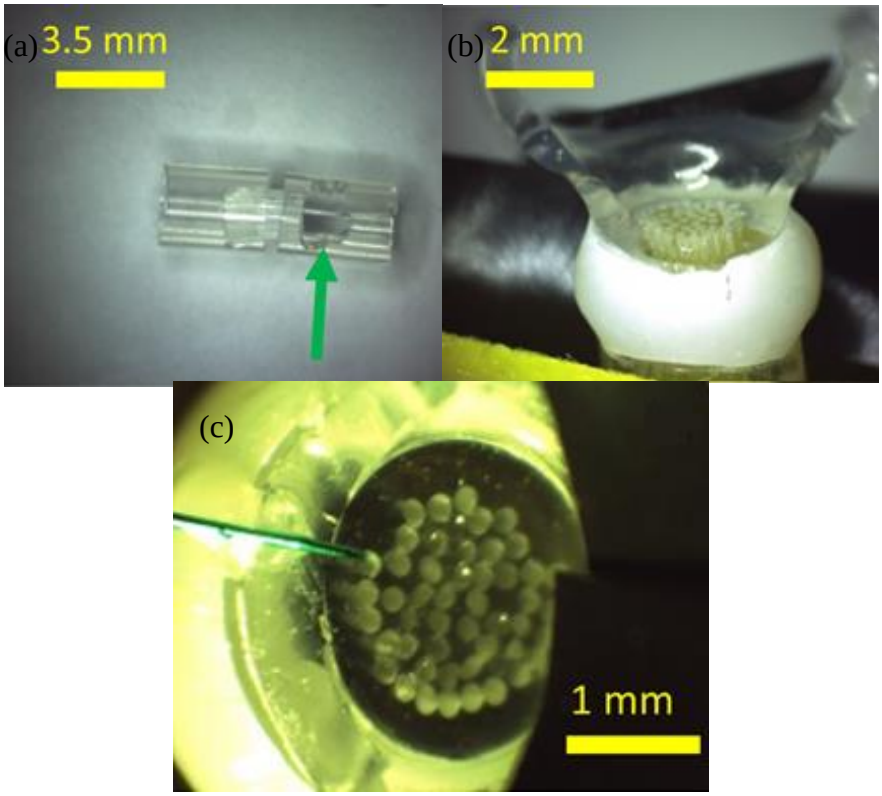

Figure 2.5: (a) a small circle with a slit leading, (b) The distal tube opened along the slit to facilitate embedding of microwires (c) placing microwires one by one inside microchannels.

The gap between the tubes was filled with a dental cement and was subjected to ultraviolet (UV) light for 8 seconds to cause it to harden. The distal tube was opened along the slit to facilitate embedding of microwires into the microchannel (Figure 2.5 (b)). 16 microwires were cut into 8 inch segments and 1 mm of insulation was trimmed off at the tips. They were then folded at 90° angles, 1 mm away from the uninsulated parts. The exposed wires were placed one by one into the microchannels through the circle made in the proximal tube and glued to the dental cement previously applied using the same technique (Figure 2.5 (c)). Dental cement was then used to seal the circle in the proximal tube, being careful not to allow any dental cement into the regenerating path of axons (Figure 2.6). All 16 wires were then braided together to make them as compact as possible and were connected subcutaneously to a head stage connector which was attached to the skull (Figure 2.7). Microwires are beneficial because they are easy to implant, permit smaller wounds, and create minimal obstruction to the regenerative path.

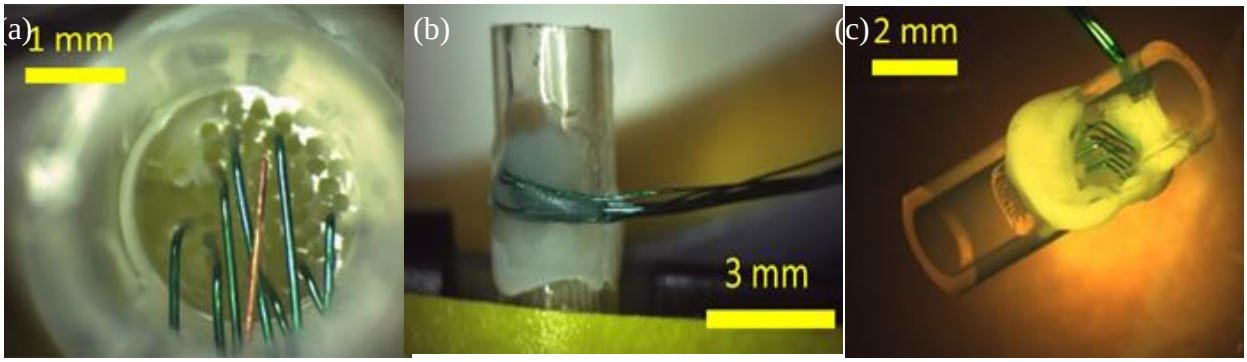

Figure 2.6: (a) 16 wires embedded inside microchannels, (b) dental cement used to secure wires to scaffold (c) the finished device.

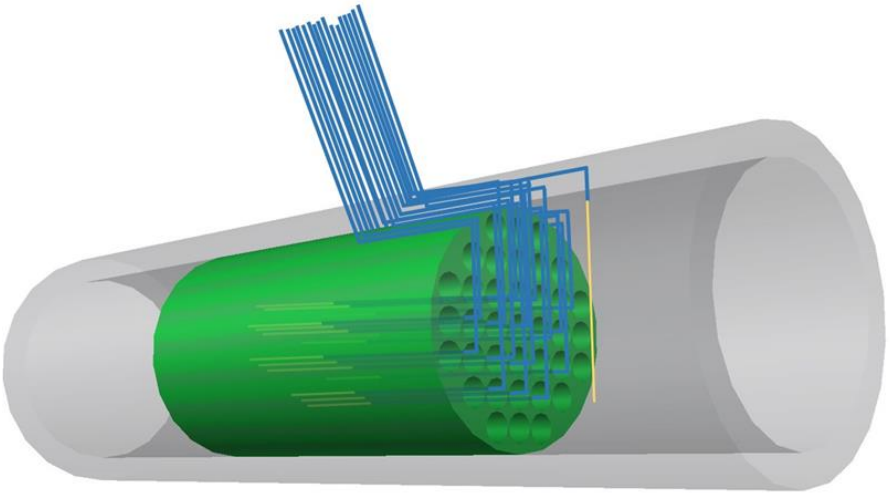

Figure 2.7: 16 wires embedded inside microchannels and one wire as a reference.

CHAPTER III

SURGICAL PROCEDURE

Surgical procedures were performed under aseptic conditions at the UTRGV Animal Facility (Figure 3.1). Prior to implantation, a Lewis rat was placed into an induction chamber and subjected to gas anesthesia (Isoflurane) until unconscious. The surgery locations (right thigh and top of head) were shaved and cleaned using a betadine scrub and isopropyl alcohol. Its maxillary central incisors were hooked into a gas mask through which it continued to receive small doses of anesthesia. It was secured to a surgery table and its body temperature was regulated with a hot pad.

Figure 3.1: Surgery setup and implementation. All surgical procedures were done under stringent ethical standards at the UTRGV animal facility.

Incisions were made along the right thigh to expose the sciatic nerve, tibialis anterior (TA), and soleus (SOL) muscles (Figure 3.2).

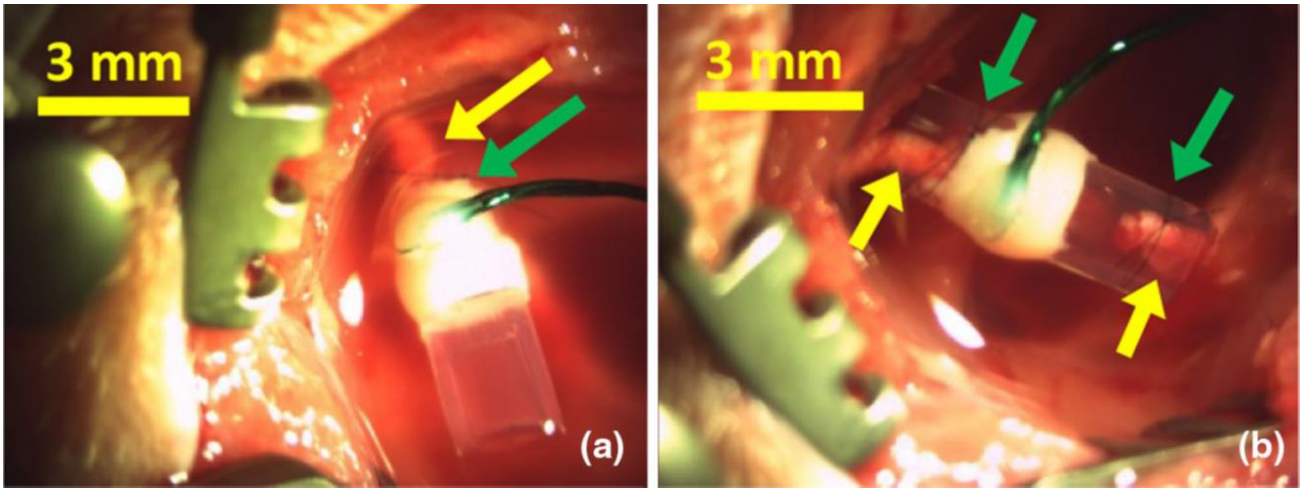

Figure 3.2: the μPNI was implanted by suturing both the distal and proximal ends of the nerves to the guides of the device. Yellow arrows indicate nerve stumps and green arrows indicate sites of surgical suture.

The nerve was severed, proximal to the tibial and fibular nerves, and the μPNI was implanted by suturing both the distal and proximal ends of the nerves to the guides of the device (Figure 3.3). EMG signals were obtained by implanting pairs of microwires (Stablohm 800A, California Fine Wires, CA) (75 μm diameter) into the TA and SOL. The whole implantable microdevice consists of a μPNI for recording placed on the transection site of the sciatic nerve, and three μCuff electrodes, one for stimulation placed on the proximal site of the transection site of the sciatic nerve and the other two for recording placed on the tibial nerve and the common peroneal nerve. Additionally, two electromyography electrode pairs were implanted on the tibialis anterior (TA) and soleus (SOL) muscles on the right hind leg to record the muscle signals during animal's locomotion tests (Figure 3.4).

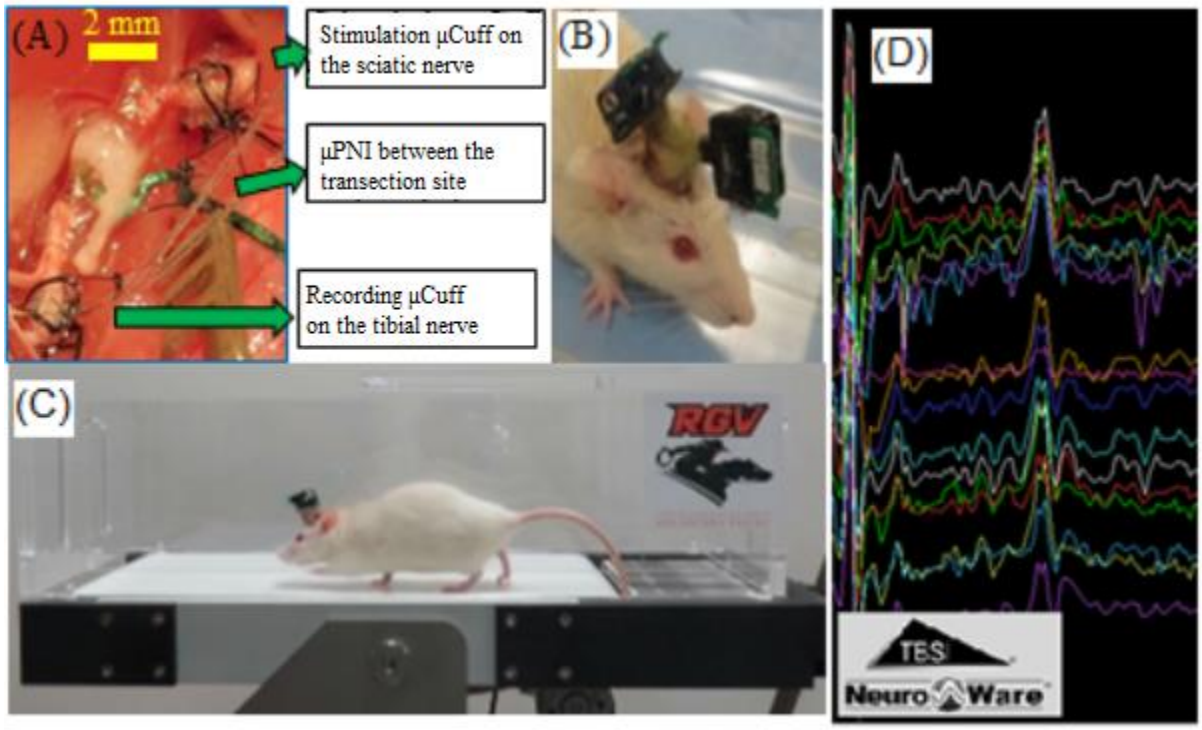

Figure 3.3: (A) Animal surgery of the sciatic nerve model. Two µCuff electrodes and µPNI are located. (B) Both TBSI stimulation and recording system headstages on a rat. (C) Video monitoring of walking locomotion. 32-channel TBSI wireless recording device is attached on the headplug (D) Neural signals from individual microwires showing different signals from each channel recorded by TBSI 32-channel wireless system. The first picks are the stimulation signals and the second picks are evoked action potentials delayed by the transition speed of the peripheral nerves. All electrodes were guided subcutaneously to an incision made at the top of the head and henceforth attached to a connector (Nano Strip Connector, A79022-001, Omnetics, MN), which was secured to the skull using dental cement and stainless steel screws.

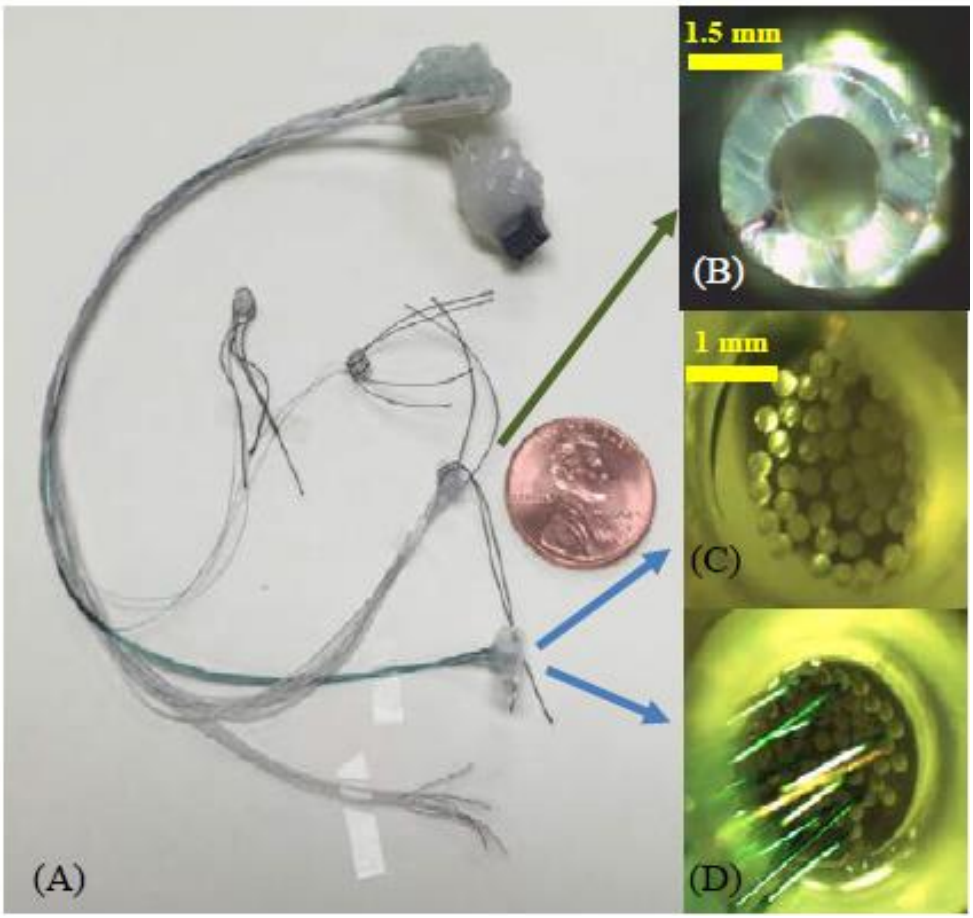

Figure 3.4: Implantable micro devices (A) whole configuration. (B) 8-electrode μCuff for stimulation. (C) 160μm diameter microchannel scaffold before inserting microwires. 16 out of 50 microchannels were occupied by microwires. (D) 16-electrode μPNI after microwires were inserted inside microchannels.

All procedures conformed to the Guide for the Care and Use of Laboratory Animals of the Institute of Laboratory Animal Resources, Commission on Life Sciences, National Research Council (National Academy Press, Washington, DC, 1996) and were reviewed and approved by the Institutional Animal Care and Use Committee UTRGV.

CHAPTER IV

RESULT

A manually fabricated implantable micro device ready for the surgery is shown in (Figure 3.4). Both an omnetics connector (Nano Strip Connector, A79022-001, Omnetics, MN) for TBSI neuroware and a sullins connector (S9009E-04-ND, 8 Position 050, Dual Row, Digi-key) for TBSI stimware were placed at one end of the microwire bundle. The other end of the microwire bundle was connected with a μPNI, three μCuffs, and two electromyography electrodes. Peripheral nerve axons were targeted in the μPNI using microchannels that isolate different groups of axons. Since the developed fabrication technique is simple and adjustable, the scaffold parameters (length and microchannel diameter) can be modified to fit different applications. (Figure 3.4C) indicates that each microchannel (160 μm diameter) is individually separated and completely sealed. This feature aims to improve the design by reducing the crosstalk between adjacent microchannels and increasing the signal-to-noise ratio. This is a significant advantage of the μPNI because other electrodes that are near each other can create crosstalk due to parasitic capacitances [90]. (Figure 3.3A) shows the successful surgery result. The μPNI was implanted between the transected sciatic nerve stumps at the location marked as ‘transection’ of the schematic design in (Figure 4.7). All embedded electrodes were routed subcutaneously and connected to a head-mounted plug (Figure 3.3B). The nerve stumps were sutured on each side of the μPNI. The stimulation μCuff was placed on the proximal sciatic nerve from the μPNI. Once the microchannel scaffolds were occupied by the regenerated nerve, the stimulation signal from the μCuff was recorded from the recording

μCuff on the tibial and the common peronial nerves. This confirmed the successful nerve regeneration through the μPNI. The μCuff electrodes were used as supplementary recording devices and contributed as a part of neural networks in the sciatic nerve branches. The electrophysiological locomotion data of the μPNI was captured by Triangle BioSystems International (TBSI, Durham, NC) wireless system (Figure 4.1).

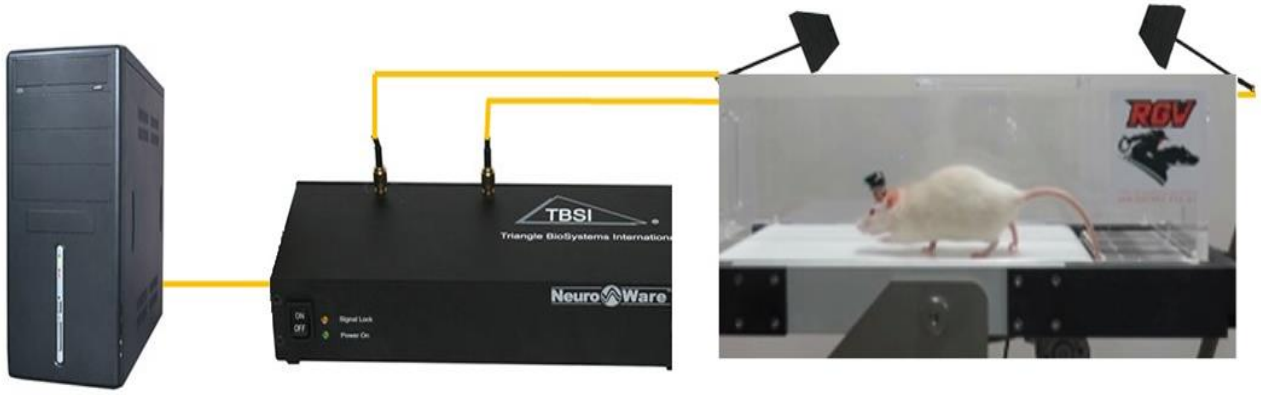

Figure 4.1: 32 channel W32 wireles system and Neuroware (Triangle BioSystems) have been used for recording.

(Figure 3.3B) shows both TBSI w-32 wireless recording system and TBSI S2W stimulator. While an animal was walking on a treadmill for behavioral pattern analysis, TBSI w-32 system recorded the electrophysiological signals from all implanted micro devices (Figure 3.3C). We used a rodent treadmill system that has the slop angle control capability (760306, Harvard Apparatus, South Natick, Massachusetts), which was installed in a procedure room at the animal facility at UTRGV. TBSI S2W stimulator was used to generate the evoked signal to analyze the neural pathways and electrophysiological properties of the sciatic nerve branches, SOL, and TA muscles. Neural recording and stimulation signals were forced to flow longitudinally within the microchannel scaffolds which make each microchannel independent from all other microchannels, making it

possible to retrieve specific signals. The implantable devices of the µPNI, the µCuff, and the EMG electrodes were implanted in the animal and neural signal recordings were obtained, while the animal was running on a treadmill. The TBSI wireless recording system gave the maximum flexibility for the locomotion studies. Due to the robust nerve regeneration of the sciatic nerve model, all channels were occupied with regenerated nerves. (Figure 3.3D) shows the electrophysiological signals captured by the 16-electrode microwire µPNI using TBSI wireless recording system three weeks after implantation. The neural signals through the regenerated nerves in the µPNI were recorded and analyzed to retrieve data corresponding to animal behavior patterns. Electrophysiological signals were recorded from all 16 electrodes (Figure 4.2). Although some signals showed were identical, these also suggested possible axonal branching from the regenerated nerves.

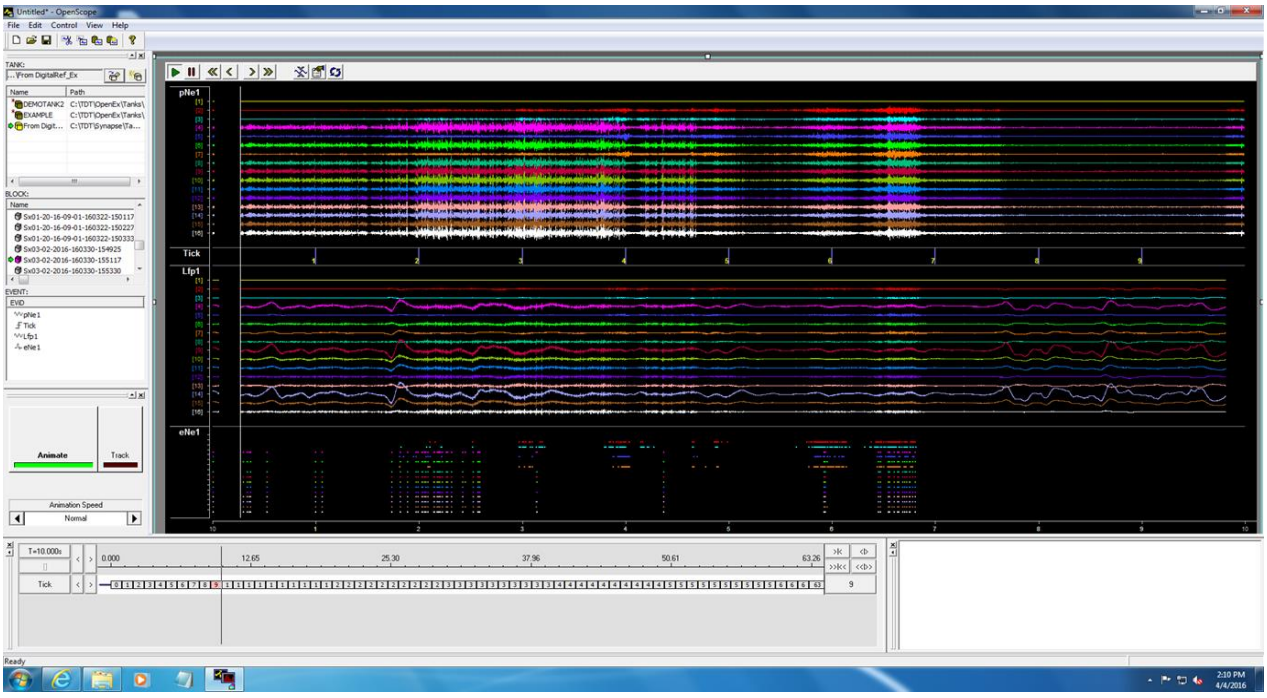

Figure 4.2: The electrophysiological signals captured by the 16-electrode microwire µPNI using TBSI wireless recording system three weeks after implantation.

The extracellular recording of neural signals consists of action potentials from several neurons near the electrode site, and background noise. Since information of the nervous system is encoded in the form of firing frequency or firing time [91], the first procedure in the interpretation of neuronal signals is the detection of the action potential firing, i.e., the neural spike. In spite of the fundamental importance of this, only a few studies on neural spike detection have appeared in the literature. In most cases, major efforts have been made to optimize experiments so that the recorded waveforms are of sufficient quality to enable reliable detection by simple traditional methods. However, situations are often encountered where the signal-to-noise ratio (SNR) of the recording is so poor as to prohibit neural spike detection using simple thresholding, and in some cases, such as the recording from a long-term implanted electrode, precise experimental control cannot be achieved. Moreover, the statistical characteristics of background noise can be very similar to those of the target signal (action potential). This statistical similarity arises from the fact that the major noise source can be electrical potentials from neurons that are not coupled sufficiently tightly to electrode sites. This "neuronal" or "biological" noise may result in more serious problems in the case of a recording from cortex or ganglia where the density of neurons can be high. This statistical similarity prohibits the satisfactory enhancement of SNR using conventional signal processing techniques such as bandpass filtering, and as a result, the detection problem becomes much more difficult to solve [92]. The processing of raw electroneurographic (ENG) recordings from the neural interface can be used to reduce noise and to estimate the neural information source. Currently, there are various electrodes under investigation as neural interfaces [92]. Their characteristics determine the choice of the signal processing method. Electrodes with limited selectivity (e.g., cuffs) can, generally, only record the compound activity formed by the superposition of action potentials belonging to many axons. Therefore, in most cases, the neural

activity recorded in this way has been used for onset detection, for example for the control of a 1-DoF hand prosthesis [93] or of FES-systems in hemiplegics Hoffer et al. (2005). Even if these limits can be partly overcome by using multi-site cuff electrodes [94] and advanced processing techniques [95], more selective PNS interfaces may be necessary to access more specific information. In fact, higher selectivity interfaces make possible the identification of single spikes from single axons (or a small group of axons) and to access the natural frequency coded information [96] in ENG signals. Among the possible choices, intraneural electrodes represent an interesting solution because of their trade-off between invasiveness and selectivity [97]. In particular, longitudinal intrafascicular electrodes (LIFEs), which are wire-based electrodes inserted longitudinally into the nerve [98], have been used in the past [99] to identify single units in multi-unit peripheral nerve recordings using different features and classification schemes. For example, artificial neural networks allowed differentiation of four to five units with a 70–90% reliability with single channel or differential recordings and a 90–98% reliability with dual channel recordings [100]. These very promising results could be improved by using different processing algorithms. For example, wavelet denoising techniques have been shown in the past to be a valuable tool for the analysis of signals recorded from the central nervous system (CNS) [101] and from the PNS during microneurography [102]. At the same time, the selectivity of intraneural electrodes (e.g., extraction of single units) enables the development of approaches based on spike sorting techniques borrowed from cortical array signal processing [103]. In (Figure 4.3) we can see some of the common methods in signal processing to remove the noises from the neural signal.

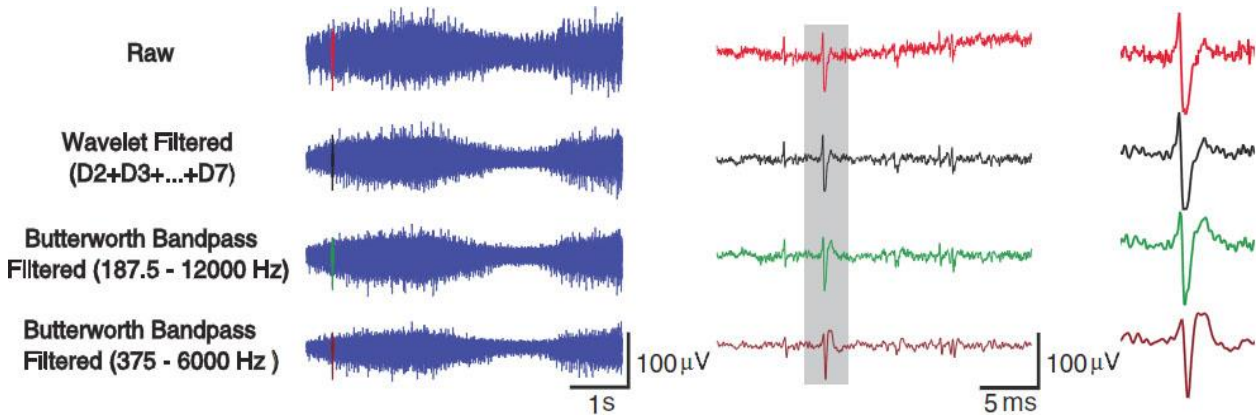

Figure 4.3: Comparison of raw, wavelet filtered (from D2 to D7, 187.5 Hz–12 kHz), and Butterworth bandpass filtered (187.5 Hz–12 kHz and 375 Hz–6 kHz) sequences from the same section of continuously intrafascicular recordings with the tfLIFE. [105].

To compare between the filtering effect on the shape of the spike waveform using the proposed approach and traditional bandpass filtering, a fourth-order Butterworth bandpass filter was used to denoise the raw signal. Two different Butterworth filters were implemented with passband frequencies between (a) 187.5 Hz–12 kHz and (b) 375 Hz–6 kHz. These bandwidths correspond to reconstruction of denoised signals using detail levels D2–D7 and D3–D6, respectively. As shown in (Figure 4.3), applying the traditional bandpass filter distorted the shape of the spike waveform. The degree of spike waveform distortion was found to become more pronounced with shrinking of the passband. In particular, the shape of the spike in the region between the first negative peak and the second positive peak was smoothed, and the duration and amplitude of the second positive peak became extended and increased [104]. The combined use of wavelet denoising and spike sorting algorithms could increase the amount of information that is decoded from intraneural recordings in the PNS. This could allow the development of more effective neuroprosthetic systems [105,106].

Here in order to remove noise from the signals, we first used notch filter for removing 60 Hz and similar interferences from the waveforms and re-referenced them to one of the 32 channels. Next we band pass filtered the signal from 300 – 5000 Hz as you can see in the (Figure 4.4).

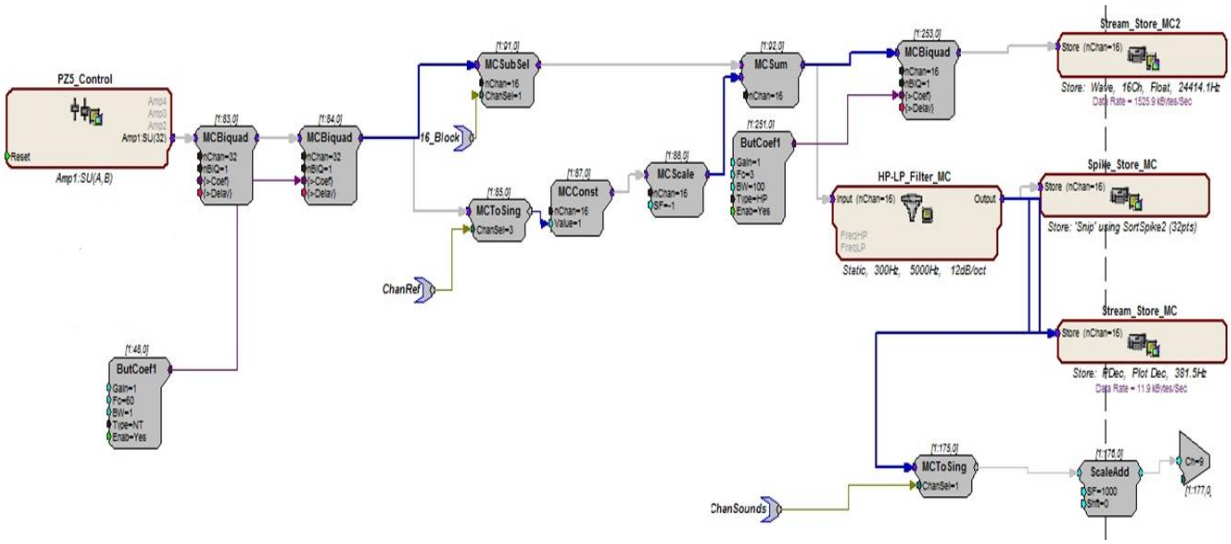

Figure 4.4: This circuit diagram shows the signal processing in order to remove the noises from the signal (TDT Synapse software has been used for signal processing).

In (Figure 4.5) and (Figure 4.6) we can see the difference in signal before denoising and after denoising. This signal processing technique greatly improved the quality of μPNI signal analyses.

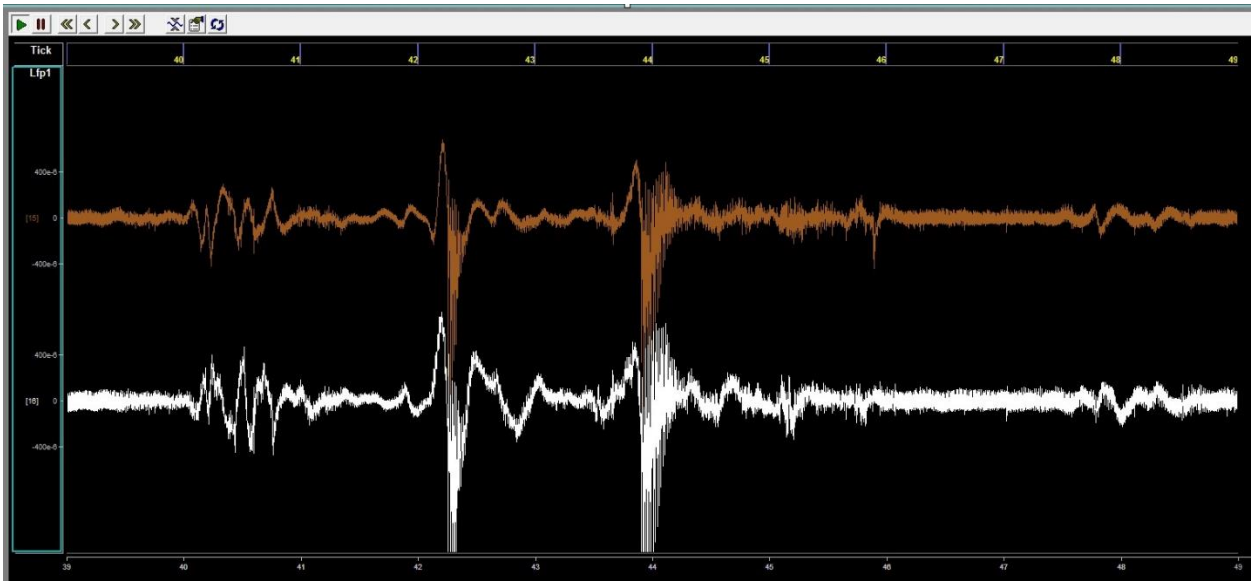

Figure 4.5: The neural signals before denoising process.

with further analysis in the future work, we could determine if the multiple axons were originated from the same parent neuron to make a same neural signal pattern. It could be confirmed by histology analysis at the end of the procedure after harvesting regenerated nerve tissues. The unique neural signal patterns of the μPNI, depending on the animal behavior patterns, will not only confirm the brain-controlled neural singnals at the μPNI, but also pioneer the delicate neuronal networks in the brain linked to the sensory and motor feedback of peripheral nerves. Action potentials with similar waveforms were identified in the locomotion microelectrode recordings and extracted using a timeamplitude window discriminator routine. The average amplitude of the action potentials extracted from microchannels was about 100 μV with amplitudes ranging from 40~200 μV (Figure 4.6). Selected and repeated action potentials comparing the μPNI, TA muscle, and cuff data were clearly demonstrating the step cycles.

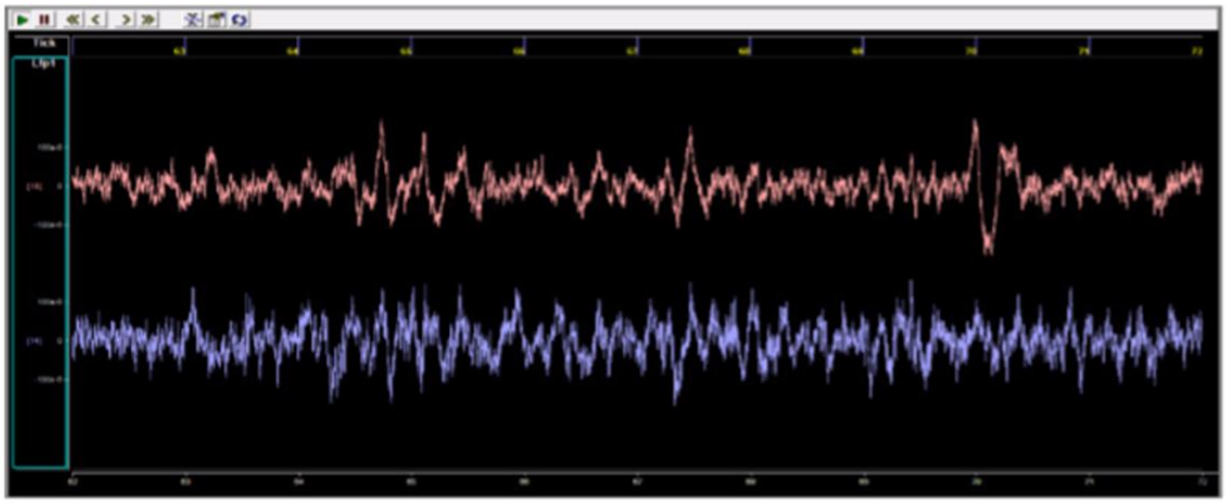

Figure 4.6: The average amplitude of the action potentials extracted from microchannels was about 100 μV with amplitudes ranging from 40~200 μV.

A neural signal combination of all microwires of the μPNI, or part of them, will express a behavioral pattern at a specific temporal moment. A repeatable behavioral pattern may express a series of temporal neural signal patterns. Thin scar tissue formation covering outside PDMS scaffolds was observed from the harvested μPNI. However, no obstructing inflammation responses was observed inside microchannels with a two-month regeneration period. PDMS is an FDA approved biomaterial for several clinical applications. As a biocompatible material, PDMS has been used in a wide range of applications, such as a structure itself as part of the device and an insulator. PDMS cuff electrodes have been used on the extradural sacral root to sense the bladder response to stimulation in patients [18].

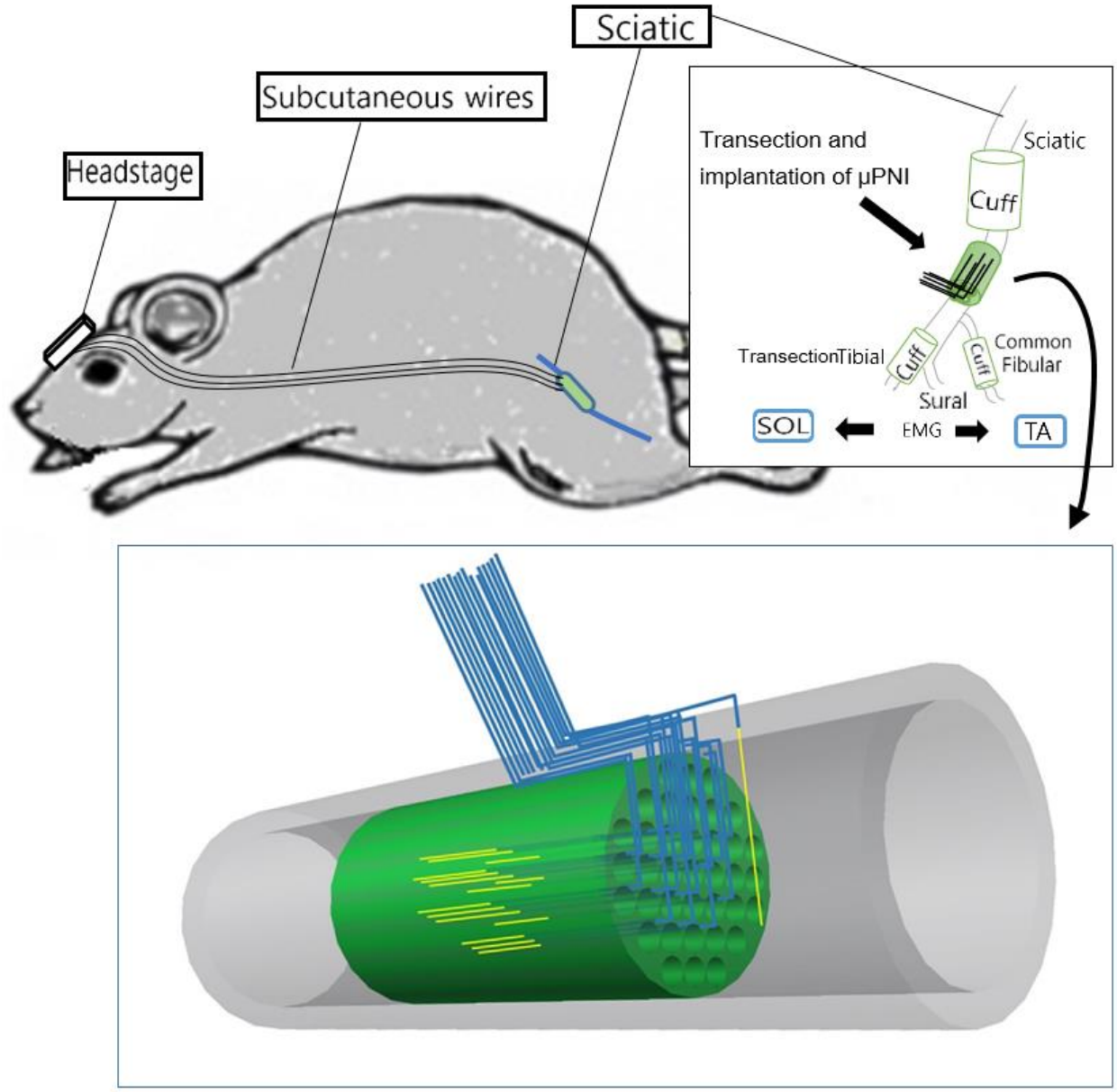

Figure 4.7: Schematic view of the animal model for µPNI, µCuff, and EMG electrodes on the sciatic nerve branches.

CHAPTER V

HISTOLOGY

Histology is the study of the microscopic anatomy of cells and tissues of plants and animals. It is commonly performed by examining cells and tissues under a light microscope or electron microscope, which have been sectioned, stained and mounted on a microscope slide. Histological studies may be conducted using tissue culture, where live human or animal cells are isolated and maintained in an artificial environment for various research projects. The ability to visualize or differentially identify microscopic structures is frequently enhanced through the use of histological stains. Histology is an essential tool of biology and medicine. can be performed manually (hand processing), but where multiple specimens have to be dealt with it is more convenient and much more efficient to use an automated tissue processing machine. These devices have been available since the 1940's and have slowly evolved to be safer in use, handle larger specimen numbers, process more quickly and to produce better quality outcomes. There are two main types of processors, the tissue-transfer machines where specimens are transferred from container to container to be processed, or the fluid transfer types where specimens are held in a single process chamber or retort and fluids are pumped in and out as required. Most modern fluid-transfer processors employ raised temperatures, effective fluid circulation and incorporate vacuum/pressure cycles to enhance processing and reduce processing times [107]. Most laboratory supervisors would emphasize to their staff the importance of tissue processing. It is

worthwhile to stress that use of an inappropriate processing schedule or the making of a fundamental mistake (perhaps in replenishing or sequencing of processing reagents) can result in the production of tissue specimens that cannot be sectioned and therefore will not provide any useful microscopic information. This can be disastrous if you are dealing with diagnostic human tissue where the whole of the specimen has been processed. There is no spare tissue. There is no diagnosis. There is however a patient to whom an explanation has to be provided. Although mechanical or electrical faults occasionally occur in tissue processors, processing mishaps where tissues are actually compromised, mainly occur because of human error. It is important to emphasize the value of proper education and training for those carrying out tissue processing and the need to apply particular care when setting up a processor for any processing run. Fresh tissue specimens will come from various sources. It should be noted that they can very easily be damaged during removal from patient or experimental animal. It is important that they are handled carefully and appropriately fixed as soon as possible after dissection. Ideally fixation should take place at the site of removal, perhaps in the operating theatre, or, if this is not possible, immediately following transport to the laboratory [108].

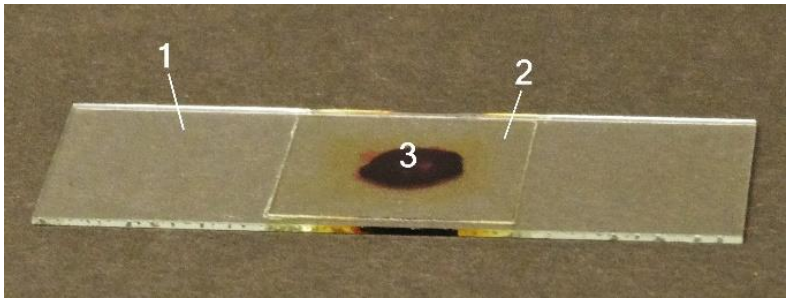

Figure 5.1: Typical histologic specimen: 1. glass microscope slide 2. glass coverslip 3. stained tissue section, mounted between 1. and 2 [132].

In order to exam the sample with confocal microscope, nerve samples were stained by using primary antibody and secondary antibody. The sample was reacted for immunofluorescent demonstration of a marker on axons, neurofilament 160 targeted by a primary antibody (NF160, 1:250 dilution, Sigma–Aldrich). The sample was then incubated overnight at 4 °C in a mixture of primary antibody and blocking solution, then washed and incubated for 1 hour at room temperature in a solution of secondary antibody, diluted 1:220 in 0.5% Triton in PBS. Goat anti-mouse IgG1 Alexa 633 was used as a secondary antibody. Finally, the sample was washed once more and dried and mounting media (Fluoromount-GTM with DAPI, eBioscience) was applied later. After histology process sample was placed on top of the glass slide and covered with cover slip. The confocal microscope images were processed using FV10-ASW 3.1 software's Z-stack function (Figure 5.2).

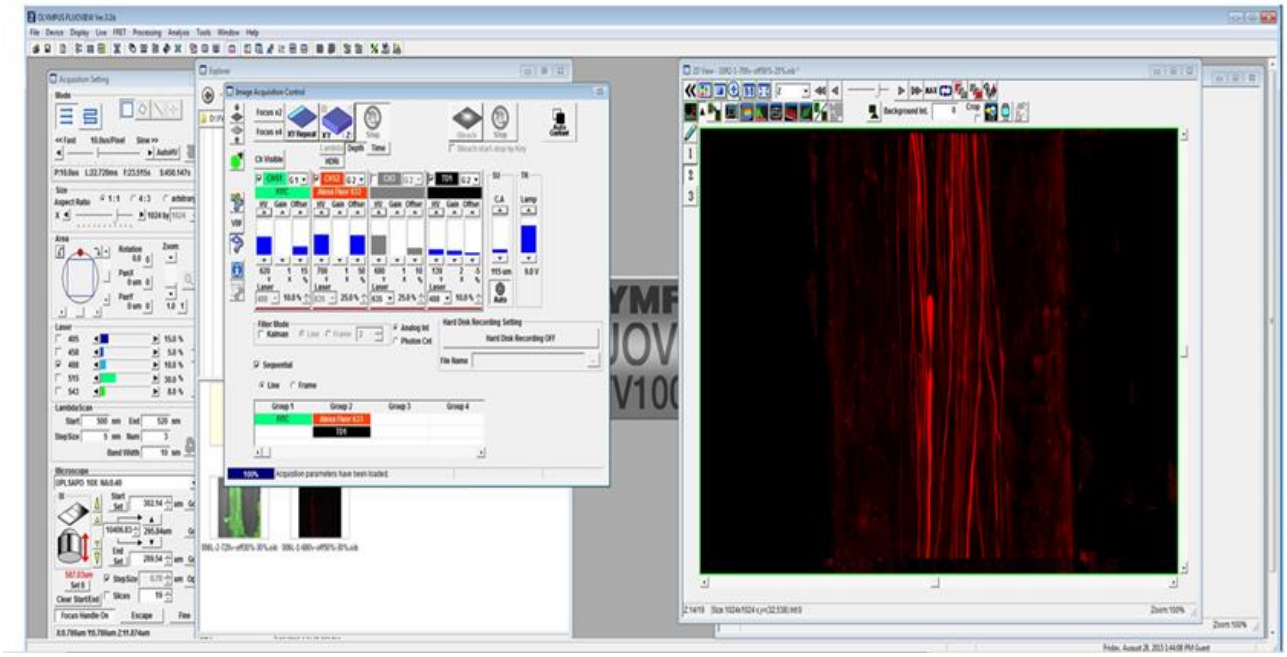

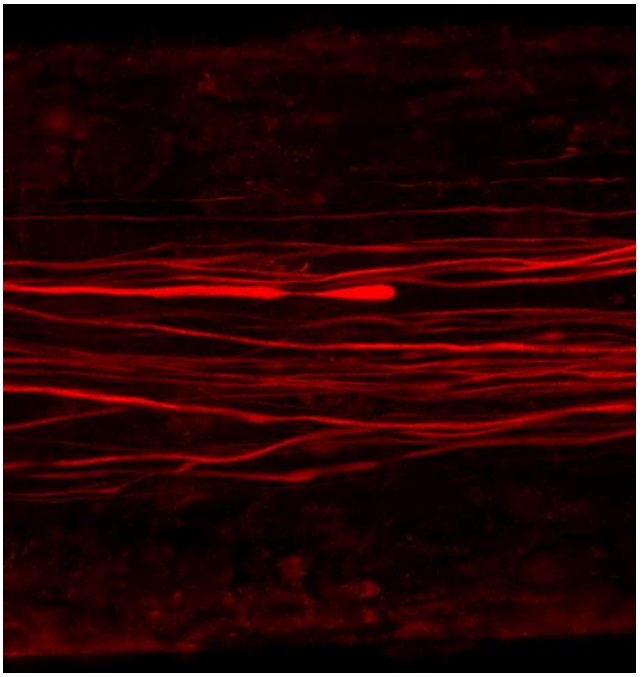

Figure 5.2: Axonal Regenerating inside the microchannel.

“Intensity projection over z axis” function was use to combine z stack pictures to observe axon lines clearly for the two dimensional figures. 160um microchannel scaffold shows 25-35 axons per microchannel when inspected using a confocal microscope (Olympus FV 1000). Confocal microscopic imaging showed the details of peripheral nerve regeneration including nerve branches and growth cones observable from within the microchannel scaffold and confirms the successful implantation of the device.

CHAPTER VI

FUTURE RESEARCH AND CONCLUSION

6.1 Conclusion

We developed unsophisticated multi microchannel nerve scaffolds and successfully implanted them in six Lewis rats supporting nerve regeneration of damaged nerves. We used PDMS as a base material for all components of the μPNI. PDMS has been widely used as a major material of the implantable devices for both research and clinical purposes [109-114], due to its easy fabrication technique and biocompatibility. To achieve translational capabilities, PDMS could be replaced by biodegradable materials, such as PCL, PLGA, and PGA [115-120]. After the nerve regeneration, the biodegradable microchannel will be dissolved to give the structures as close to a natural nerve as possible. Each biodegradable material needs to be tested for its own biocompatibility and degradation rate in the peripheral nerve model. A cross sectional view shows how the scaffold can have different diameter microchannels within it by using different sized microwires in the PDMS micro molding (Figure 7.1a, b) the former is a bright field image and the latter is a scanning electron microscope (SEM) image. This allows for flexibility in choosing from a variety of design configurations that target specific nerve fibers.

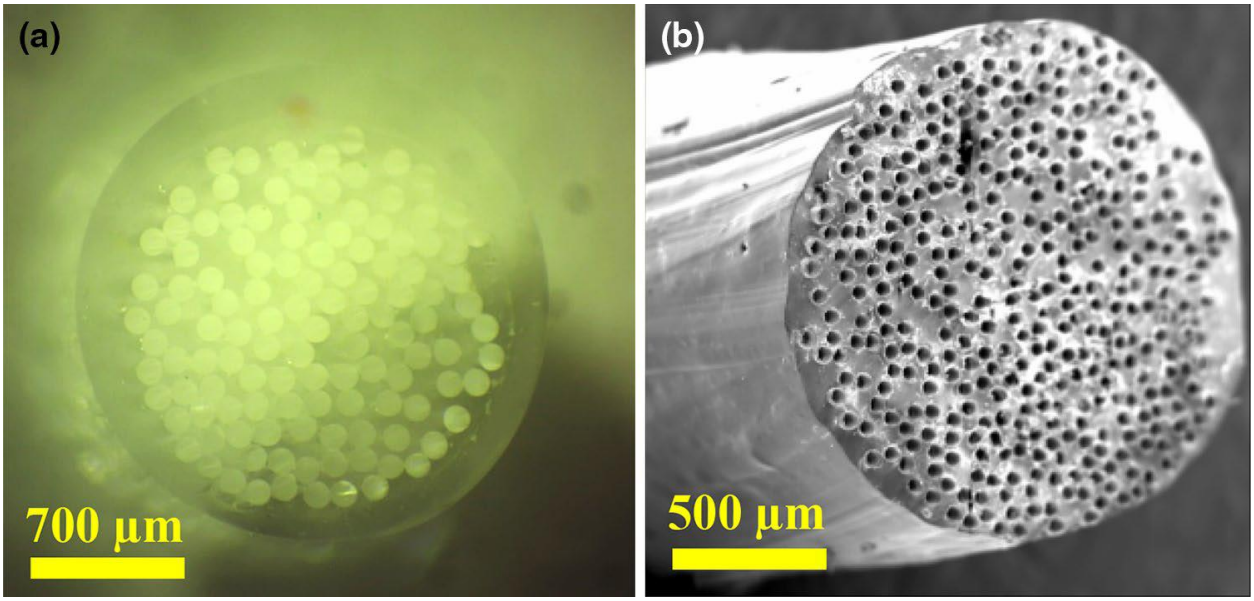

Figure 6.1: Cross sectional view of (a) bright field image and (b) SEM image of scaffold; designing microchannels of different sizes is easily attained by using wire of varying thicknesses. Adjusting the size can be used to target either efferent or afferent axons.

The structure of the scaffold can be easily modified to more closely match conditions that encourage the greatest amount of regeneration of neural tissue. Microchannels with small diameters can be used to isolate individual axons by restricting the space allotted for regeneration. Other axons would thereby be forced to enter other microchannels. The µPNI has been developed and successfully implanted in the rat sciatic nerves. The microelectrodes were long enough to record neural activity from the source of the neural signal (Nodes of Ranvier) with high selectivity. From the analysis the microchannels of the device, it was observed that an increasingly amount of axons are present at the distal ends of the tibial, sural, and peroneal nerves confirming the success of the device. Additionally, multichannel nerve scaffold in combination with IHC and confocal microscopy allowed the limited identification of axon types and growth patterns of peripheral nerve regeneration in three dimensional detail, including examples of both

growth cones and axonbranching, toward the direction of individual channels. The proposed handcrafted multichannel nerve scaffold will be able to repair multiple injured nerves during a single surgery with a higher guarantee of reestablishing nerve functionality not only for the peripheral nervous system but also can be applicable to other applications.

6.2 Future Research

For the chronic animal studies, the microdevices need to be implanted securely inside the animal body without biological rejection and mechanical failure. Moreover, minimally invasive surgery is always required. A biological reaction to foreign materials could be significant in any chronic animal study requiring implantation, especially those that require the implanted device to be kept for more than three months. We recorded electrophysiological signals with the μPNI for two months period, since the axonal reinnervation was achieved after one month and stable muscle signals could be captured afterward. Many implantable devices have been used in the everyday clinical practice and decades of implantation is not a significant issue anymore, which makes us confident about the chronic studies. Though we have developed the μPNI targeting the sciatic nerve model with gait analysis of the somatic nervous system, it can be easily adapted for other nerve models including the modulation of the autonomic nervous system. The developed fabrication technique of the μPNI is not dependent on the nerve size as any size of the μPNI components can be developed, ranging from few hundred micrometers to several millimeters in diameter which covers almost all major peripheral nerves and their branches. This allows for flexibility in choosing from a variety of design configurations that target specific nerve fibers. The μPNI has a significant potential as neuroscience research test beds, if it is combined with biochemical neurotropic factors. The microchannels of the μPNI can be coated with different

neurotropic factors to separate the growth of sensory or motor specific axons into the microchannels. They will encapsulate multiple neurotropic factors, such as nerve growth factor (NGF) [121], neurotrophin-3 (NT-3) [122-124], brain-derived neurotrophic factor (BDNF) [125,126], and neurotrophin 4/5 (NT-4/5) [127], ciliary neurotrophic factor (CNTF), and glial cell line-derived neurotrophic factor (GDNF). Inducing the specific axonal growth from a microchannel structure to biochemically infused microchannels could provide data for a more in-depth analysis of axon growth behavior.

REFERENCES

[1] Ziegler-Graham, K., et al. "Estimating the prevalence of limb loss in the United States: 2005 to 2050." Archives of physical medicine and rehabilitation 89.3 (2008): 422-429.

[2] Custom Prosthetics, Artificial Limbs (http://www.progoandp.com/services/prosthetics).

[3] No. 1705: A 3000-Year-Old Toe". Uh.edu. 2004-08-01. Retrieved 2013-03-13. (http://www.uh.edu/engines/epi1705.htm).

[4] Hubbard, Sharon, Douglas G. Smith, and Jeffrey M. Gambel. "Prosthetic cost projections for servicemembers with major limb loss from Vietnam and OIF/OEF." Journal of rehabilitation research and development 47.4 (2010): 387.

[5] Cost of a Prosthetic Limb. Cost Helper Health. Retrieved 13 April 2015. (http://health.costhelper.com/prosthetic-legs.html)

[6] Stubblefield, Kathy A., et al. "Occupational therapy protocol for amputees with targeted muscle reinnervation." Journal of rehabilitation research and development 46.4 (2009): 481.

[7] Brain-controlled prosthetic arm connected to nerves. ScienceNordic. October 13, 2014 (http://sciencenordic.com/brain-controlled-prosthetic-arm-connected-nerves).

[8] How Prosthetic Limbs Work. HowStuffWorks, a division of InfoSpace LLC (http://science.howstuffworks.com/prosthetic-limb.htm)

[9] Boundless. “Structure of a Nerve.” Boundless Anatomy and Physiology. Boundless, 21 Jul. 2015. Retrieved 10 Apr. 2016. (https://www.boundless.com/physiology/textbooks/boundless-anatomy-and-physiology-textbook/peripheral-nervous-system-13/nerves-130/structure-of-a-nerve-695-1700/)

[10] Topp, Kimberly S., and Benjamin S. Boyd. "Structure and biomechanics of peripheral nerves: nerve responses to physical stresses and implications for physical therapist practice." Physical therapy 86.1 (2006): 92-109.

[11] Navarro, X., Krueger, T. B., Lago, N., Micera, S., Stieglitz, T. and Dario, P. (2005), A critical review of interfaces with the peripheral nervous system for the control of neuroprostheses and hybrid bionic systems. Journal of the Peripheral Nervous System, 10: 229–258. doi: 10.1111/j.1085-9489.2005. 10303.x

[12] Dhillon GS, Lawrence SM, Hutchinson DT, Horch KW (2004) Residual function in peripheral nerve stumps of amputees: implications for neural control of artificial limbs. J Hand Surg Am 29: 605-615.

[13] Kuiken TA, Li G, Lock BA, Lipschutz RD, Miller LA, Stubblefield KA, et al. (2009) Targeted Muscle Reinnervation for Real-Time Myoelectric Control of Multifunction Artificial Arms. JAMA 301: 619–628.

[14] Rossini PM, Micera S, Benvenuto A, Carpaneto J, Cavallo G, et al. (2010) Double nerve intraneural interface implant on a human amputee for robotic hand control. Clin Neurophysiol 121: 777-783.

[15] Agnew SP, Schultz AE, Dumanian GA, Kuiken TA (2012) Targeted reinnervation in the transfemoral amputee: a preliminary study of surgical technique. Plast Reconstr Surg 129: 187-194.

[16] Badia J, Boretius T, Andreu D, Azevedo-Coste C, Stieglitz T, et al. (2011) Comparative analysis of transverse intrafascicular multichannel, longitudinal intrafascicular and multipolar cuff electrodes for the selective stimulation of nerve fascicles. J Neural Eng 8: 036023.

[17] Tyler DJ, Durand DM (2002) Functionally selective peripheral nerve stimulation with a flat interface nerve electrode. IEEE Trans Neural Syst Rehabil Eng 10:294-303.

[18] A Grill WM, Mortimer JT (2000) Neural and connective tissue response to long term implantation of multiple contact nerve cuff electrodes. J Biomed Mater Res 50: 215-226.

[19] Serra J, Bostock H, Navarro X (2010) Microneurography in rats: a minimally invasive method to record single C-fiber action potentials from peripheral nerves in vivo. Neurosci Lett 470: 168-174.

[20] Lawrence SM, Dhillon GS, Jensen W, Yoshida K, Horch KW (2004) Acute peripheral nerve recording characteristics of polymer-based longitudinal intrafascicular electrodes. IEEE Trans Neural Syst Rehabil Eng 12: 345-348.

[21] Lawrence SM, Dhillon GS, Jensen W, Yoshida K, Horch KW (2004) Acute peripheral nerve recording characteristics of polymer-based longitudinal intrafascicular electrodes. IEEE Trans Neural Syst Rehabil Eng 12: 345-348.

[22] Branner A, Stein RB, Fernandez E, Aoyagi Y, Normann RA (2004) Long-term stimulation and recording with a penetrating microelectrode array in cat sciatic nerve. IEEE Trans Biomed Eng 51: 146-157.

[23] Thurgood BK, Warren DJ, Ledbetter NM, Clark GA, Harrison RR (2009) A wireless integrated circuit for 100-channel charge-balanced neural stimulation. IEEE Trans Biomed Circuits Syst 3: 405-414.

[24] Normann RA (2007) Technology insight: future neuroprosthetic therapies for disorders of the nervous system. Nat Clin Pract Neurol 3: 444-452.

[25] Navarro X, Calvet S, Rodríguez FJ, Stieglitz T, Blau C, et al. (1998) Stimulation and recording from regenerated peripheral nerves through polyimide sieve electrodes. J Peripher Nerv Syst 3: 91-101.

[26] Ceballos D, Valero-Cabré A, Valderrama E, Schüttler M, Stieglitz T, et al. (2002) Morphologic and functional evaluation of peripheral nerve fibers regenerated through polyimide sieve electrodes over long-term implantation. J Biomed Mater Res 60: 517-528.

[27] Lago N, Ceballos D, Rodríguez FJ, Stieglitz T, Navarro X (2005) Long term assessment of axonal regeneration through polyimide regenerative electrodes to interface the peripheral nerve. Biomaterials 26: 2021-2031.

[28] Castro J, Negredo P, Avendaño C (2008) Fiber composition of the rat sciatic nerve and its modification during regeneration through a sieve electrode. Brain Res 1190: 65-77.

[29] Cho SH, Lu HM, Cauller L, Romero Ortega MI, Lee JB, et al. (2008) Biocompatible SU-8-Based Microprobes for Recording Neural Spike Signals from Regenerated Peripheral Nerve Fibers. IEEE Sensors Journal 8: 1830-1836.

[30] Garde K, Keefer E, Botterman B, Galvan P, Romero MI (2009) Early interfaced neural activity from chronic amputated nerves. Front Neuroeng 2: 5.20.

[31] FitzGerald JJ, Lago N, Benmerah S, Serra J, Watling CP, et al. (2012) A regenerative microchannel neural interface for recording from and stimulating peripheral axons in vivo. J Neural Eng 9: 016010.

[32] Vallbo A, Hagbarth K, Torebjo rk H, Wallin G (1979). Somatosensory, proprioceptive, and sympathetic activity in human peripheral nerves. Physiol Rev 59:919–957.

[33] Gandevia SC, Hales JP (1997). The methodology and scope of human microneurography. J Neurosci Methods 74:123–136.

[34] Ochoa JL, Torebjo¨ rk JR (1983). Sensations evoked by intraneural microstimulation of single mechanoreceptor units innervating the human hand. J Physiol 342:633–654.

[35] Shimojo M, Suzuki T, Namiki A, Saito T, Kunimoto M, Makino R, Ogawa H, Ishikawa M, Mabuchi K (2003). Development of a system for experiencing tactile sensation from a robot hand by electrically stimulating sensory nerve fiber. Proceedings of the IEEE International Conference on Robotics and Automation, pp 1263–1270.

[36] Smit JP, Rutten WL, Boom HB (1999). Endoneural selective stimulating using wire-microelectrode arrays. IEEE Trans Rehabil Eng 7:399–412.

[37] Veltink PH, van Alste JA, Boom HB (1989). Multielectrode intrafascicular and extraneural stimulation. Med Biol Eng Comput 27:19–24.

[38] Drake KL, Wise KD, Farraye J, Anderson DJ, BeMent SL (1988). Performance of planar multisite microprobes in recording extracellular single-unit intracortical activity. IEEE Trans Biomed Eng 35:719–732.

[39] Ehrfeld W, Munchmeyer D (1991). LIGA method, three dimensional microfabrication using synchrotron radiation. Nucl Instrum Methods Phys Res A 303:523–531.

[40] Normann RA, Maynard EM, Rousche PJ, Warren DJ (1998). A neural interface for a cortical vision prosthesis. Vision Res 12:2577–2587.

[41] Yoon TH, Hwang EJ, Shin DY, Park SI, Oh SJ, Jung SC, Shin HC, Kim SJ (2000). A micromachined silicon depth probe for multichannel neural recording. IEEE Trans Biomed Eng 47:1082–1087.

[42] Stieglitz T, Gross M (2002). Flexible BIOMEMS with electrode arrangements on front and back side as key component in neural prostheses and biohybrid systems. Sensors Actuators B 12:1–7.

[43] Takeuchi S, Suzuki T, Mabuchi K, Fujita H (2004). 3D flexible multichannel neural probe array. J Micromech Microeng 14:104–107.

[44] Hetke JF, Lund JL, Najafi K, Wise D, Anderson DJ (1994). Silicon ribbon cables for chronically implantable microelectrode arrays. IEEE Trans Biomed Eng 41:314–321.

[45] Hoogerwerf AC, Wise KD (1994). A 3D micro-electrode array for chronic neural recording. IEEE Trans Biomed Eng 41:1136–1146.

[46] Kim C, Wise KD (1996). A 64-site multishank CMOS low-profile neural stimulating probe. IEEE J Solid State Circuits 31:1230–1238.

[47] Kipke DR, Vetter RJ, Williams JC, Hetke JF (2003). Silicon-substrate intracortical microelectrode arrays for long-term recording of neuronal spike activity in cerebral cortex. IEEE Trans Rehabil Eng 11:151–155.

[48] Najafi K, Hetke JF (1990). Strength characterization of silicon microprobes in neurophysiological tissues. IEEE Trans Biomed Eng 37:474–481.

[49] Arts HA, Jones DA, Anderson DJ (2003). Prosthetic stimulation of the auditory system with intraneural electrodes. Ann Otol Rhinol Laryngol 112:20–25.

[50] McCreery D, Pikov V, Lossinsky A, Bullara L, Agnew W (2004). Arrays for chronic functional microstimulation of the lumbosacral spinal cord. IEEE Trans Neural Syst Rehabil Eng 12:195–207.

[51] Gonzalez C, Rodriguez M (1997). A flexible perforated microelectrode array probe for action potential recording in nerve and muscles tissues. J Neurosci Methods 72:189–195.

[52] Stieglitz T, Meyer JU (1997). Microtechnical interfaces to neurons.Microsyst Technol Chem Life Sci pp 131–162.

[53] Nordhausen CT, Maynard EM, Normann RA (1996). Single unit recording capabilities of a 100 microclectrode array. Brain Res 726:129–140.

[54] Rutten WLC, Smit JPA, Frieswijk TA, Bielen JA, Brouwer ALH, Buitenweg JR, Heida C (1999). Neuro-electronic interfacing with multielectrode arrays. IEEE Eng Med Biol Mag 18:47–55.

[55] Rutten WLC, Smit JPA, Rozijn TH, Meier JH (1995). 3D neuroelectronic interface devices for neuromuscular control: design studies and realisation steps. Biosens Bioelectron 10:141–153.

[56] Rutten WLC (2002). Selective electrical interfaces with the nervous system. Ann Rev Biomed Eng 4:407–452.

[57] Branner A, Stein RB, Normann RA (2001). Selective stimulation of cat sciatic nerve using an array of varying-length microelectrodes. J Neurophysiol 85:1585–1594.

[58] Branner A, Normann RA (2000). A multielectrode array for intrafascicular recording and stimulation in sciatic nerve of cats. Brain Res Bull 51:293–306.

[59] Branner A, Stein RB, Fernandez E, Aoyagi Y, Normann RA (2004). Long-term stimulation and recording with a penetrating microelectrode array in cat sciatic nerve. IEEE Trans Biomed Eng 51:146–157.

[60] Aoyagi Y, Stein RB, Branner A, Pearson KG, Normann RA (2003). Capabilities of a penetrating microelectrode array for recording single units in dorsal root ganglia of the cat. J Neurosci Methods 128:9–20.

[61] Warwick K, Gasson M, Hutt B, Goodhew I, Kyberd P, Andrews B, Teddy P, Shad A (2003). The application of implant technology for cybernetic systems. Arch Neurol 60:1369–1373.

[62] Llinas R, Nicholson C, Johnson K (1973). Implantable monolithic wafer recording electrodes for neurophysiology. In: Brain Unit Activity During Behaviour. Phillips MI (Ed). Charles Thomas, IL, pp 105–110.

[63] Edell DJ (1986). A peripheral nerve information transducer for amputees: long-term multichannel recordings from rabbit peripheral nerves. IEEE Trans Biomed Eng 33:203–214.

[64] Kovacs GTA, Storment CW, Rosen JM (1992). Regeneration microelectrode array for peripheral nerve recording and stimulation. IEEE Trans Biomed Eng 39:893–902.

[65] Dario P, Garzella P, Toro M, Micera S, Alavi M, Meyer U, Valderrama E, Sebastiani L, Ghelarducci B, Mazzoni C, Pastacaldi P (1998). Neural interfaces for regenerated nerve stimulation and recording. IEEE Trans Rehabil Eng 6:353–363.

[66] Rosen JM, Grosser M, Hentz VR (1990). Preliminary experiments in nerve regeneration through laser-drilled holes in silicon chips. Restor Neurol Neurosci 2:89–102.

[67] Navarro X, Calvet S, Buti´ M, Go´mez N, Cabruja E, Garrido P, Villa R, Valderrama E (1996). Peripheral nerve regeneration through microelectrode arrays based on silicon technology. Restor Neurol Neurosci 9:151–160.

[68] Mannard A, Stein RB, Charles D (1974). Regeneration electrode units: implants for recording from single peripheral nerve fibers in freely moving animals. Science 183:547–549.

[69] Akin T, Najafi K, Smoke RH, Bradley RM (1994). A micromachined silicon sieve electrode for nerve regeneration applications. IEEE Trans Biomed Eng 41:305–313.

[70] Kovacs GTA, Storment CW, Halks-Miller M, Belczynski CR, Della Santina CC, Lewis ER, Maluf NI (1994). Silicon-substrate microelectrode array for parallel recording of neural activity in peripheral and cranial nerves. IEEE Trans Biomed Eng 41:567–577.

[71] Wallman L, Zhang Y, Laurell T, Danielsen N (2001). The geometric design of micromachined silicon sieve electrodes influences functional nerve regeneration. Biomaterials 22: 1187–1193.

[72] Bradley RM, Cao X, Akin T, Najafi K (1997). Long term chronic recordings from peripheral sensory fibers using a sieve electrode array. J Neurosci Methods 73:177–186.

[73] Della Santina CC, Kovacs GTA, Lewis ER (1997). Multi-unit recording from regenerated bullfrog eighth nerve using implantable silicon-substrate microelectrodes. J Neurosci Methods 72:71–86.

[74] Mensinger AF, Anderson DJ, Buchko CJ, Johnson MA, Martin DC, Tresco PA, Silver RB, Highstein SM (2000). Chronic recording of regenerating VIIIth nerve axons with a sieve electrode. J Neurophysiol 83:611–615.

[75] Zhao Q, Drott J, Laurell T, Wallman L, Lindstro¨m K, Bjursten LM, Lundborg G, Montelius L, Danielsen N (1997). Rat sciatic nerve regeneration through a micromachined silicon chip. Biomaterials 18:75–80.

[76] Navarro X, Calvet S, Rodri´guez FJ, Stieglitz T, Blau C, Buti´ M, Valderrama E, Meyer JU (1998). Stimulation and recording from regenerated peripheral nerves through polyimide sieve electrodes. J Peripher Nerv Syst 2:91–101.

[77] Ceballos D, Valero-Cabre´ A, Valderrama E, Schu¨ ttler M, Stieglitz T, Navarro X (2002). Morphological and functional evaluation of peripheral nerve fibers regenerated through polyimide sieve electrodes over long term implantation. J Biomed Mater Res 60:517–528.

[78] Lago N, Ceballos D, Rodri´guez FJ, Stieglitz T, Navarro X (2005). Long term assessment of axonal regeneration through polyimide regenerative electrodes to interface the peripheral nerve. Biomaterials 26:2021–2031.

[79] Klinge PM, Vafa MA, Brinker T, Brandes A, Walter GF, Stieglitz T, Samii M, Wewetzer K (2001a). Molecular characterization of axonal sprouting and tissue changes after long-term implantation of a polyimide sieve electrode to the transected adult rat sciatic nerve. Biomaterials 22:2333–2343.

[80] Negredo P, Castro J, Lago N, Navarro X, Avendan˜ o C (2004). Differential growth of axons from sensory and motor neurons through a regenerative electrode: a stereological, retrograde tracer, and functional study in the rat. Neuroscience 128:605–615.

[81] Riso RR (1999). Strategies for providing upper extremity amputees with tactile and hand position feedback moving closer to the bionic arm. Technol Health Care 7:401–409.

[82] Loeb GE, Marks WB, Beatty PG (1977). Analysis and microelectrode design of tubular electrode arrays intended for chronic, multiple single-unit recording from captured nerve fibres. Med Biol Eng Comput 15:195–201.

[83] Wells MR, Vaidya U, Ricci JL, Christie C (2001). A neuromuscular platform to extract electrophysiological signals from lesioned nerves: a technical note. J Rehabil Res Dev 38:385–390.

[84] Gore RK, Choi Y, Bellamkonda R, English A (2015) Functional recordings from awake, behaving rodents through a microchannel based regenerative neural interface. J Neural Eng 12: 016017.

[85] Choi Y, Gore RK, English AW, Bellamkonda RV (2012) Multilumen PDMS scaffolds for peripheral nerve repair and interface. In: the 40th Neural Interfaces Conference, Salt Lake City, UT, 2012.

[86] Choi Y, Park S, Chung Y, Gore RK, English AW, et al. (2014) PDMS microchannel scaffolds for neural interfaces with the peripheral nervous system. In: The 27th IEEE International Conference on Micro Electro Mechanical Systems (MEMS 2014), San Francisco, CA.

[87] Choi Y, Shafqat F, Heo H, Bellamkonda RV (2012) Development of micro channel nerve grafts and their application in peripheral nerve regeneration. In: 2012 International Annual Symposium on Regenerative Rehabilitation, Pittsburgh, PA.

[88] Gore RK, Choi Y, English AW, Bellamkonda RV (2012) Peripheral neural recordings in awake and behaving rats after sciatic regeneration through a microchannel based neural nterface. In: Neuroscience 2012, Society for Neuroscience 42nd annual meeting, New Orleans, LA.

[89] Hossain R, Kim B, Pankratz R, Ajam A, Park S, et al. (2015) Handcrafted multilayer PDMS microchannel scaffolds for peripheral nerve regeneration. Biomed Microdevices 17: 109.

[90] Takei K, Kawano T, Kawashima T, Sawada K, Kaneko H, et al. (2010) Microtube-based electrode arrays for low invasive extracellular recording with a high signal-to-noise ratio. Biomed Microdevices 12: 41-48.

[91] F. Rieke, D. Warland, R. De Ruyter van Steveninck, and W. Bialek, Spikes: Exploring the Neural Code. Cambridge, MA: MIT Press, 1996.

[92] Kim, Kyung Hwan, and Sung June Kim. "A wavelet-based method for action potential detection from extracellular neural signal recording with low signal-to-noise ratio." Biomedical Engineering, IEEE Transactions on 50.8 (2003): 999-1011.

[93] X. Navarro, T.B. Krueger, N. Lago, S. Micera, T. Stieglitz, P. Dario A critical review of interfaces with the peripheral nervous system for the control of neuroprostheses and hybrid bionic systems J Peripher Nerv Syst, 10 (3) (2005), pp. 229–258.

[94] R.B. Stein, D. Charles, J.A. Hoffer, J. Arsenault, L.A. Davis, S. Moorman, et al. New approaches for the control of powered prostheses particularly by high-level amputees Bull Prosthet Res, 10–33 (1980), pp. 51–62.

[95] P.B. Yoo, D.M. Durand Selective recording of the canine hypoglossal nerve using a multicontact flat interface nerve electrode IEEE Trans Biomed Eng, 52 (8) (2005), pp. 1461–1469.

[96] C.C.K. Lin, M.S. Ju, H.S. Cheng Model-based ankle joint angle tracing by cuff electrode recordings of peroneal and tibial nerves Med Biol Eng Comput, 45 (4) (2007), pp. 375–385.

[97] Micera S, Carrozza M, Beccai L, Vecchi F, Dario P. Hybrid bionic systems for the replacement of hand function. IEEE Proc 2006;94(10)1752–62.

[98] K. Yoshida, R.B. Stein Characterization of signals and noise rejection with bipolar longitudinal intrafascicular electrodes IEEE Trans Biomed Eng, 46 (2) (1999), pp. 226–234.

[99] L.J. Li, J. Zhang, F. Zhang, W.C. Lineaweaver, T.Y. Chen, Z.W. Chen Longitudinal intrafascicular electrodes in collection and analysis of sensory signals of the peripheral nerve in a feline model Microsurgery, 25 (7) (2005), pp. 561–565.

[100] E.V. Goodall, K.W. Horch Separation of action potentials in multiunit intrafascicular recordings IEEE Trans Biomed Eng, 39 (3) (1992), pp. 289–295.

[101] T.G. McNaughton, K.W. Horch Action potential classification with dual channel intrafascicular electrodes IEEE Trans Biomed Eng, 41 (7) (1994), pp. 609–616.

[102] K.G. Oweiss, D.J. Anderson Noise reduction in multichannel neural recordings using a new array wavelet denoising algorithm Neurocomputing, 38–40 (2001), pp. 1687–1693.

[103] A. Diedrich, W. Charoensuk, R.J. Brychta, A.C. Ertl, R. Shiavi Analysis of raw microneurographic recordings based on wavelet de-noising technique and classification algorithm: wavelet analysis in microneurography IEEE Trans Biomed Eng, 50 (1) (2003), pp. 41–50.

[104] Z. Nenadic, J.W. Burdick Spike detection using the continuous wavelet transform IEEE Trans Biomed Eng, 52 (1) (2005), pp. 74–87.

[105] Qiao, Shaoyu, et al. "Stationary wavelet transform and higher order statistical analyses of intrafascicular nerve recordings." Journal of neural engineering 9.5 (2012): 056014.

[106] Citi, Luca, et al. "On the use of wavelet denoising and spike sorting techniques to process electroneurographic signals recorded using intraneural electrodes." Journal of neuroscience methods 172.2 (2008): 294-302.

[107] Clayden EC. Practical section cutting and staining. Edinburgh: Churchill Livingstone, 1971.

[108] Geoffrey Rolls, An Introduction to Specimen Processing, Leica Biosystems Nussloch GmbH 2016.

[109] Kurstjens GaM, Borau A, Rodriguez A, Rijkhoff NJM, Sinkjaer T (2005) Intraoperative recording of electroneurographic signals from cuff electrodes on extradural sacral roots in spinal cord injured patients. The Journal of Urology 174: 1482–1487.

[110] Stöver T, Lenarz T (2009) Biomaterials in cochlear implants. GMS Curr Top Otorhinolaryngol Head Neck Surg 8: Doc10.

[111] Malcolm RK, Edwards KL, Kiser P, Romano J, Smith TJ (2010) Advances in microbicide vaginal rings. Antiviral Res 88 Suppl 1: S30-39.

[112] Grill WM, Craggs MD, Foreman RD, Ludlow CL, Buller JL (2001) Emerging clinical applications of electrical stimulation: opportunities for restoration of function. J Rehabil Res Dev 38: 641-653.

[113] Martens FM, Heesakkers JP (2011) Clinical results of a brindley procedure: sacral anterior root stimulation in combination with a rhizotomy of the dorsal roots. Adv Urol 2011: 709708.

[114] Andriot M, Degroot JV, Meek J, Meeks R, Gerlach E, et al (2007) Silicones in Industrial Applications. Inorganic Polymers, RD Jaeger and M. Gleria, Eds ed: Nova Science Publishers pp. 61-161.

[115] Sivak WN, Bliley JM, Marra KG (2014) Polymeric Biomaterials for Nerve Regeneration: Fabrication and Implantation of a Biodegradable Nerve Guide. In: Axon Growth and Regeneration A. J. Murray, Ed ed: Springer pp. 139-148.

[116] Liu JJ, Wang CY, Wang JG, Ruan HJ, Fan CY (2011) Peripheral nerve regeneration using composite poly (lactic acid-caprolactone)/nerve growth factor conduits prepared by coaxial electrospinning. Journal of Biomedical Materials Research Part A 96A: 13-20.

[117] Nectow AR, Marra KG, Kaplan DL (2012) Biomaterials for the development of peripheral nerve guidance conduits. Tissue Eng Part B Rev 18: 40-50.

[118] Kehoe S, Zhang XF, Boyd D (2012) FDA approved guidance conduits and wraps for peripheral nerve injury: a review of materials and efficacy. Injury 43: 553-572.

[119] Mobasseri A, Faroni A, Minogue BM, Downes S, Terenghi G, et al. (2015) Polymer scaffolds with preferential parallel grooves enhance nerve regeneration. Tissue Eng Part A 21: 1152-1162.

[120] Sterne GD, Brown RA, Green CJ, Terenghi G (1997) Neurotrophin-3 delivered locally via fibronectin mats enhances peripheral nerve regeneration. Eur J Neurosci 9: 1388-1396.

[121] Reid AJ1, de Luca AC, Faroni A, Downes S, Sun M, et al. (2013) Long term peripheral nerve regeneration using a novel PCL nerve conduit. Neurosci Lett 544: 125-130.

[122] Lotfi P, Garde K, Chouhan AK, Bengali E, Romero-Ortega MI (2011) Modality specific axonal regeneration: toward selective regenerative neural interfaces. Frontiers in Neuroengineering 4: 11-11.

[123] Yamauchi J, Chan JR, Miyamoto Y, Tsujimoto G, Shooter EM (2005) The neurotrophin-3 receptor TrkC directly phosphorylates and activates the nucleotide exchange factor Dbs to enhance Schwann cell migration. Proc Natl Acad Sci U S A 102: 5198-5203.

[124] Sahenk Z, Oblinger J, Edwards C (2008) Neurotrophin-3 deficient Schwann cells impair nerve regeneration. Exp Neurol 212: 552-556.

[125] Utley DS, Lewin SL, Cheng ET, Verity AN, Sierra D, et al. (1996) Brain-derived neurotrophic factor and collagen tubulization enhance functional recovery after peripheral nerve transection and repair. Arch Otolaryngol Head Neck Surg 122: 407-413.

[126] Sendtner M, Holtmann B, Kolbeck R, Thoenen H, Barde YA (1992) Brainderived neurotrophic factor prevents the death of motoneurons in newborn rats after nerve section. Nature 360: 757-759.

[127] Liu X, Jaenisch R (2000) Severe peripheral sensory neuron loss and modest motor neuron reduction in mice with combined deficiency of brain-derived neurotrophic factor, neurotrophin 3 and neurotrophin 4/5. Dev Dyn 218: 94-101.

[128] Dumanian, Gregory A., et al. "Targeted reinnervation for transhumeral amputees: current surgical technique and update on results." Plastic and reconstructive surgery 124.3 (2009): 863-869.

[129] Kuiken, Todd A., et al. "Prosthetic command signals following targeted hyper-reinnervation nerve transfer surgery." *Engineering in Medicine and Biology Society, 2005. IEEE-EMBS 2005. 27th Annual International Conference of the*. IEEE, 2005.

[130] Miller, Laura A., et al. "Control of a six degree of freedom prosthetic arm after targeted muscle reinnervation surgery." *Archives of physical medicine and rehabilitation* 89.11 (2008): 2057-2065.

[131] Study Blue - Nervous System (https://www.studyblue.com/#flashcard/view/8819508).

[132] Histology (http://en.wikipedia.org/wiki/Histology)

BIOGRAPHICAL SKETCH

Ali Ajam was born on April 20, 1992 in Mashhad, Iran. He attended The Ferdowsi University of Mashhad from 2010 to 2014 and graduated with Bachelor of Science degree in Electrical Engineering in 2014. He attended University of Texas Rio Grande Valley from 2015-2016 and graduated with a Master of Science degree in Electrical Engineering in 2016. Currently, he is a Research Assistant in department of Electrical Engineering and has presented a number of conference papers in NeuroRegeneration Collaborative Conference at Rice University and has published a number of papers in the journals such as Biomedical Microdevices (BMMD) and Sensor Network and Data Communications. His research is mostly focused on regenerative peripheral nerve interface that facilitate a direct connection between the nervous system and external technologies such as limb prosthetics or data acquisition systems for further processing. Prior to that he was mainly working on designing FPGA architectural diagrams and developing VHDL to implement the design functionality. Upon graduation from the University of Texas Rio Grande Valley, Ali Ajam is looking forward to beginning PhD program in the United States.

Permanent address: 941 N Sugar Road, Edinburg, Texas, USA

Permanent email address: ali.ajam90@yahoo.com